Geosci. Model Dev. Discuss., 8, 53–140, 2015
www.geosci-model-dev-discuss.net/8/53/2015/
doi:10.5194/gmdd-8-53-2015

Geoscientific
Model Development
Discussions
Open Access

EMPOWER-1.0: an Efficient Model of Planktonic ecOsystems WrittEn in R

T. R. Anderson[1], **W. C. Gentleman**[2], **and A. Yool**[1]

[1]National Oceanography Centre, University of Southampton, Waterfront Campus, European Way, Southampton SO14 3ZH, UK
[2]Department of Engineering Mathematics, Dalhousie University, 5269 Morris St., Halifax, Nova Scotia, B3H 4R2, Canada

Received: 10 November 2014 – Accepted: 2 December 2014 – Published: 5 January 2015

Correspondence to: T. R. Anderson (tra@noc.ac.uk)

Published by Copernicus Publications on behalf of the European Geosciences Union.

Abstract

Modelling marine ecosystems requires insight and judgement when it comes to deciding upon appropriate model structure, equations and parameterisation. Many processes are relatively poorly understood and tough decisions must be made as to how to mathematically simplify the real world. Here, we present an efficient plankton modelling testbed, EMPOWER-1.0, coded in the freely available language R. The testbed uses simple two-layer "slab" physics whereby a seasonally varying mixed layer which contains the planktonic marine ecosystem is positioned above a deep layer that contains only nutrient. As such, EMPOWER-1.0 provides a readily available and easy to use tool for evaluating model structure, formulations and parameterisation. The code is transparent and modular such that modifications and changes to model formulation are easily implemented allowing users to investigate and familiarise themselves with the inner workings of their models. It can be used either for preliminary model testing to set the stage for further work, e.g., coupling the ecosystem model to 1-D or 3-D physics, or for undertaking front line research in its own right. EMPOWER-1.0 also serves as an ideal teaching tool. In order to demonstrate the utility of EMPOWER-1.0, we carried out both a parameter tuning exercise and structural sensitivity analysis. Parameter tuning was demonstrated for four contrasting ocean sites, focusing on Station India in the North Atlantic (60° N, 20° W), highlighting both the utility of undertaking a planned sensitivity analysis for this purpose, yet also the subjectivity which nevertheless surrounds the choice of which parameters to tune. Structural sensitivity tests were then performed comparing different equations for calculating daily depth-integrated photosynthesis, as well as mortality terms for both phytoplankton and zooplankton. Regarding the calculation of daily photosynthesis, for example, results indicated that the model was relatively insensitive to the choice of photosynthesis–irradiance curve, but markedly sensitive to the method of calculating light attenuation in the water column. The work highlights the utility of EMPOWER1.0, and simple models in general, as a means of comprehending, diagnosing and formulating equations for the dynamics of marine ecosystems.

1 Introduction

Ecosystem models are ubiquitous in marine science today, used to study a range of compelling topics including ocean biogeochemistry and its response to changing climate, end-to-end links from physics to fish and associated trophic cascades, the impact of pollution on the formation of harmful algal blooms, etc. Models have become progressively elaborated in recent years, a consequence of both superior computing power and an expanding knowledge base from field studies and laboratory experiments. All manner of models have appeared in the published literature varying in terms of structure, equations and parameterisation. Anderson et al. (2014), for example, commented on the “enormous” diversity seen in chosen formulations for dissolved organic matter (DOM) in the current generation of marine ecosystem models and asked whether reliable simulations can be expected given this diversity. This question applies not just to modelling DOM, but also to most processes and components considered in modern marine ecosystem modelling.

A certain amount of variability among models is to be expected because of differing objectives among modelling studies. A distinction can, for example, be made between models designed primarily for improving understanding of system dynamics, as opposed to those for out-and-out prediction (Anderson, 2010). Ultimately, however, much of the variability seen in model structure and equations is an outcome of personal choice on the part of the practitioner. Indeed, the art of modelling is in making decisions regarding model structure, parameters, design of simulations, types of output analysis, etc. The underlying root of this diversity and seeming subjectivity is that, despite a wealth of available data, many processes in marine ecosystems are not easy to characterise mathematically. Modellers therefore need to consider how this uncertainty affects their results and use it to inform how best to construct and parameterise their models for chosen applications. Sensitivity analysis and model validation are the obvious means to address model uncertainty, as well as model intercomparison studies. There is however an additional problem, namely that ocean biology is inextricably linked to physics and both incur modelling error. An appropriate physical framework must be selected that adequately represents mixing, advection and the seasonal changes in the depth of the upper mixed layer. Understandably, 1- or 3-dimensional physical frameworks are the usual choice, given the realism thus provided. But this increased dimensionality (or spatial resolution) comes at a price. They require expertise and time to set up, sufficient computational resources for running and storage of output and, last but not least, analysis of the frequently copious output into coherent results, which can be a major undertaking. These constraints serve to limit the extent to which modellers can and do carry out extensive diagnosis and testing of their models including sensitivity analysis and validation.

In the early days of marine ecosystem modelling, it was necessary to resort to simple empirical approaches to deal with physics given the limited power of computers at the time. The so-called zero-dimensional "slab" models that came to the fore were the cornerstone of their discipline in the mid 20th century. Slab models have a simple physical structure consisting of two vertical layers. The depth of the upper (mixed) layer, which can vary seasonally, was determined empirically from observations of vertical profiles of temperature or density. Containing the pelagic marine ecosystem, the upper layer was positioned above an essentially implicit (in that it is unchanging) bottom layer that contains a (typically fixed) nutrient concentration. Such slab models can be run quickly and straightforwardly, enabling both a multitude of runs and ease of analysing results.

Despite the simplicity of the two-layer slab physics, these models are sufficiently well formulated to permit realistic and insightful simulations of marine ecosystems (e.g., Evans and Parslow, 1985; Fasham et al., 1990). Indeed, looking back at the history of marine ecosystem modelling, it is remarkable how simple models allowed so much progress to be made, notably by pioneers such as Gordon Riley, John Steele and Mike Fasham (Gentleman, 2002). Of course, we admire these individuals when it came to encapsulating the complexity of the real world with mathematical equations. They necessarily had to think deeply about their models because they had to build them from scratch as, in most instances, established relationships for processes such as photosynthesis, grazing and mortality could not be borrowed from elsewhere. A key aspect of their success, we submit, is that they experimented extensively with their models, trying out different formulations and parameterisations in order to see the effect on model predictions (e.g., Anderson and Gentleman, 2012). It is this preparation that served them so well, allowing them to set up meaningful simulations from which they could so effectively draw conclusions and make progress in their field of study.

The need for preparation in terms of exploring sensitivity to ecosystem model formulations and parameterisation is no less in the modern era, indeed it is arguably greater given our deeper knowledge of the marine biota and a correspondingly larger multitude of mathematical formulations to choose from. We propose that modellers can benefit from extensively “playing with” and testing their models and that the use of simple slab physics is an obvious choice in this regard, at least for ocean locations where the bulk of the biological activity occurs in the surface mixed layer. Experimentation of this kind may then be used to set the stage for the “serious” model runs that may follow, e.g. in 1-D or 3-D, although it is also entirely possible to undertake successful studies using only slab physics models. In addition, because they are straightforward to understand and do not require powerful computing resources to run, such simple models are ideal for use in teaching future generations of marine scientists about ecological structure and function.

Here, we present a slab a.k.a. zero-dimensional, and hence computationally efficient, plankton ecosystem testbed, coded in the freely available R environment, EMPOWER-1.0: Efficient Model of Planktonic ecOsystems WrittEn in R. Our aim is to provide EMPOWER-1.0 for general use and to demonstrate how it can readily and easily be used both to study ecosystem dynamics at a range of ocean sites and to assess the pros and cons of different model choices for best representing and analysing the ecosystems in question. EMPOWER’s code is structured in a modular way to ensure maximum ease of adjusting parameters and formulations and, indeed, the inclusion of entirely new marine ecosystem compartments, processes and associated outputs as required. This study is structured as follows. First, a brief history of slab models in marine science is presented to illustrate the origin and utility of these models as research tools in marine science. A simple representative nutrient-phytoplankton-zooplankton-detritus (NPZD) model is then described and implemented within EMPOWER. The utility of EMPOWER as a testbed for undertaking model parameterisation is then demonstrated by a parameter adjustment exercise, specifically the fitting of the NPZD model to observed seasonal cycles of chlorophyll and nutrients at each of four stations in diverse regions of the world ocean. The sensitivity analysis is then extended to model equations with a comparison of the performance of different equations for calculating, first, daily depth-integrated photosynthesis and, second, phytoplankton and zooplankton mortality. Finally, the utility of slab models is discussed in context of ongoing contemporary marine ecosystem modelling research.

2 Slab models: from pioneering studies to the present day

In this section, we provide a history of slab modelling which serves as an introduction to how these models are constructed, as well as to demonstrate that, despite their simplicity, the simulations these models generate can be meaningful and realistic. Models provide the theoretical basis for our understanding of the dynamics of marine ecosystems. One of the first applications of theory in biological oceanography occurred around 80 years ago when scientists were interested in the mechanisms driving the spring phytoplankton bloom that is characteristic of many marine systems. The basic theory as we know it today, whereby bloom initiation occurs as the water column stratifies, was proposed in the early 1930s by Haaken H. Gran, a Norwegian botanist (Gran, 1932; Gran and Braarud, 1935). Mathematical testing of this proposal was essential in order to establish quantitative merit, given the dynamic interplay between bottom-up controls on phytoplankton via light and nutrients vs. top-down control by grazing. Following on from initial work by Fleming (1939), it was Gordon Riley, a biological oceanographer based at the Bingham Oceanographic Laboratory in the northeastern USA, who constructed a model of seasonal phytoplankton dynamics for Georges Bank (Riley, 1946), a remarkable achievement at the time (Anderson and Gentleman, 2012). The model had a single differential equation for the rate of change of phytoplankton biomass, expressed with terms for photosynthesis, respiration and grazing. Using a photoysnthesis–irradiance (*P*–*I*) curve based on his own ship-board experiments, Riley developed a formula for daily depth-averaged photosynthesis in the mixed-layer that was derived from observed seasonal irradiance at the ocean surface as calculated by atmospheric transmission by Kimball (1928), measured light attenuation coefficients and a nutrient limitation term. The seasonal cycle of mixed layer depth was imposed empirically, with calculated photosynthesis in the euphotic zone being diminished accordingly when mixed layer depth (MLD) exceeded that of the euphotic zone (Fig. 1). Temperature was considered to affect net primary production via regulation of respiration. Despite its simplicity, in both biology and physics, Riley's model successfully reproduced the spring plankton bloom at Georges Bank, highlighting the subtle interplay between growth and grazing in controlling plankton stocks.

Although Riley's model considered depth-averaged photosynthesis over the mixed layer, it could not be described as a slab model per se because it did not account for fluxes of material across the pycnocline. It was John Steele, a mathematical marine biologist from Scotland, who took the next step by experimenting with a dynamic ecosystem embedded within multi-layer models (e.g., Steele, 1956), arguably a coarser version of what is done today in the more complex 1-D models. Steele's experience with this model led him to realise that much of the net effect of vertical gradients could be captured with just a few layers, and he further simplified the physics to a two-layer sea in his study of the plankton in the North Sea (Steele, 1958). The resulting NPZ ecosystem was confined to the upper layer with a lower layer that contained only nutrient, in fixed concentration. Inputs of nutrients to the surface layer occurred due to mixing, balanced by export via phytoplankton sinking and mixing (Fig. 2). Steele had thus constructed the first slab model of its kind although with this, as well as his later models including those in his seminal work *The Structure of Marine Ecosystems* (Steele, 1974), he used a fixed, rather than seasonally-varying, mixed layer depth. Applying the model to study the plankton of Fladen Ground and other regions in the northern North Sea, Steele demonstrated good agreement between the model and estimates of production from observations. Through work such as this, Steele emphasised that it is simplification that allows us to most easily address the controlling factors in marine ecosystems. One of Steele's best-remembered findings, demonstrated again using simple models, is that the form of the zooplankton closure term has important consequences for ecosystem dynamics and export flux (Steele and Henderson, 1992). This finding remains relevant to modellers today and, indeed, we will examine model sensitivity to zooplankton mortality in Sect. 4.4.

It was Geoff Evans and John Parslow who would make the next major advance in the development of slab models with their "model of annual plankton cycles" (Evans and Parslow, 1985). Following Steele, they opted for an NPZ ecosystem embedded within the same two-layer framework with the marine ecosystem restricted to the upper layer and a fixed nutrient concentration in the lower. Evans and Parslow provided a more complete representation of the interaction of the marine ecosystem with its physical environment by allowing the depth of the mixed layer to vary seasonally with direct impacts on the model state variables. As the mixed layer deepens, nutrients are entrained from below while phytoplankton density is diluted because their surface layer biomass is spread over a greater depth. Conversely, as the mixed layer shallows, the concentrations of nutrients and phytoplankton are unchanged although losses occur on a per unit area (m^{-2}) basis. As many zooplankton can swim, Evans and Parslow assumed that they are able to avoid detrainment in a similar manner to the assumptions of prior models (e.g. Steele, 1958; Riley et al., 1949), as well as mixing, in which case their concentration increases as MLD decreases.

Evans and Parslow (1985) also took seasonal and daily irradiance forcing into consideration, in combination with depth integration of a non-linear *P*–*I* curve. As opposed to previous studies that had used observations, variation in light at the ocean surface was calculated from standard trigonometric/astronomical formulae (Brock, 1981), with transmission losses in the atmosphere as 70 % of cloud cover and photosynthetically active radiation (PAR) as 3/8 of total irradiance. Variation in light with time of day was assumed to be triangular (Steele, 1962), permitting analytic integration in time. A notable contribution of Evans and Parslow's (1985) paper is the appendix which provides the equations required to construct a model subroutine to calculate daily depth-integrated photosynthesis in a model layer as a function of noon irradiance (PAR entering the layer from above), day length, phytoplankton concentration, rate of light extinction (Beer's law) and parameters for maximum photosynthesis and initial slope that define the P–I curve.

In common with their predecessors, Evans and Parslow were interested in the factors controlling the initiation of the spring phytoplankton bloom, focussing on the role of vertical mixing. Bloom initiation, they concluded, required a low rate of primary production over winter, which is to be expected in the North Atlantic due to deep mixed layers at that time, and is also linked to coupling between phytoplankton and grazers. The simplicity of the slab model was key to their conclusions as articulated in their own words: "It is worth emphasising the advantages of analysing simple models, and simplifying models until they can be analysed". The controls on phytoplankton dynamics in high-nutrient low-chlorophyll (HNLC) areas such as the Subarctic Pacific has remained a topical issue ever since, in large part because limitation by iron is also indicated (Martin et al., 1994; Coale et al., 1996), but the role of grazing and the link between phytoplankton-zooplankton coupling and mixed layer depth remains firmly established as a key mechanism in these systems (Frost, 1987; Fasham, 1995; Chai et al., 2000; Smith and Lancelot, 2004).

Perhaps the most famous slab modelling paper, published five years after Evans and Parslow (1985), is the study of nitrogen cycling in the Sargasso Sea by Fasham et al. (1990; henceforth FDM90). It is by far the most highly cited marine ecosystem model (Arhonditsis et al. (2006) noted that it had accumulated 405 ISI cites by November 2005; this number has increased to 737 as of November 2014). In terms of physical structure, Fasham's model used the same basic slab construct as in Evans and Parslow

(1985), with seasonally varying mixed layer depth and irradiance forcing. The novel aspects of FDM90 were instead related to additional complexity of the ecosystem, expanding from a simple NPZ to explicitly separate new and regenerated production by including state variables for nitrate and ammonium (critical for calculating the f ratio; Eppley and Peterson, 1979), as well as having a simple microbial loop of dissolved organic nitrogen and bacteria. Sinking detritus was also added as a state variable, facilitating the prediction of export flux. The success of this model was due to it being the first attempt to fully elucidate the processes involved in the recycling of nitrogen in the euphotic zone, as well as the complimentary roles of zooplankton and bacteria. The simplified physics of the model allowed it to be run on PCs of that era and Fasham purportedly distributed the code on floppy disks, allowing other researchers to run the model on their PCs.

The description of the marine ecosystem provided by FDM90 has largely served as the foundation for marine ecosystem modelling ever since. With the advent of increasing computer power, as well as increasing interest in the spatio-temporal behaviour of plankton systems, most modelling studies are now undertaken in 1-D or 3-D physical frameworks. Nevertheless, many slab modelling studies have been published since FDM90 which follow the basic design described above, or slight modifications thereof (Table 1). A range of ecosystem models of varying complexity have been incorporated within slab physics and applied to contrasting sites throughout the world ocean. The basic physical construction is similar in most cases consisting of a classic slab structure with a seasonal cycle of mixed layer depth specified from data and seasonal irradiance from standard trigonometric equations. Remarkably, Evans and Parslow's (1985) equations for calculating daily depth-integrated photosynthesis have prevailed and been used in most studies. A more sophisticated calculation method was developed by Morel (1988, 1991) and a simplified form of this (Anderson, 1993) is examined in Sect. 4.3. The models in Table 1 have been used for a diverse range of applications including studies of parameter optimisation (Spitz et al., 1998; Fennel et al., 2001; Schartau et al., 2001; Hemmings et al., 2004), parameter sensitivity analysis (Mitra, 2009; Mitra et al., 2007, 2014), phytoplankton bloom dynamics (Findlay et al., 2006), nutrient cycling via organic and inorganic pathways (Llebot et al., 2010), primary production in HNLC systems (Kidston et al., 2013) and primary production and export flux in contrasting regions (Fasham, 1995; Onitsuka and Yanagi, 2005).

3 Model description

We demonstrate the use of EMPOWER-1.0 using a simple NPZD ecosystem model and forcing for four time series stations in the ocean. The code is readily adapted to incorporate other ecosystem models, including the relatively complex models of the modern era, and/or forcing for other ocean sites.

3.1 Slab setup and forcing

The model uses slab physics as per Evans and Parslow (1985), namely a seasonally varying surface mixed layer that contains the ecosystem positioned above a deep homogeneous layer containing unchanging nutrient and no plankton (Fig. 2). We have also included temperature dependencies for the physiological rates in the ecosystem model (see below). Our model was set up for four stations, two in the North Atlantic (stations India, 60° N, 20° W and Biotrans, 47° N, 20° W) and two HNLC systems (station Papa in the north Pacific, 50° N, 145° W and Kerfix in the Southern Ocean, 50°40′ S, 68°25′ E). These stations were chosen because of their contrasting environments, as illustrated by the differences in forcing variables: seasonally varying mixed layer depth (MLD), irradiance (I) and sea surface temperature (T) (Fig. 3), as well as deep nitrate (N_0; see below). Mixed layer depths were taken from World Ocean Atlas (Antonov et al., 2010; Locarnini et al., 2010). In common with most previous slab modelling studies, noon (peak daily) irradiance at the ocean surface for a given latitude as a function of time of year is calculated using standard trigonometric/astronomical equations. The effect of clouds on atmospheric transmission was calculated using the model of Reed

(1977). The equations for irradiance forcing are not usually provided as part of published model descriptions but, for completeness, they are listed here in Appendix A.

The bottom layer in most slab models is assumed to have a fixed concentration of nutrient, N_0. There is in reality a gradient of nutrient with depth and this can be represented empirically in slab models using simple functions of nutrients vs. depth (Frost, 1987; Steele and Henderson, 1993; Fasham, 1995). We adopted this approach here for stations India and Biotrans, using simple linear relationships with depth:

$$N_0(z) = a_N \mathrm{MLD} + b_N \tag{1}$$

The regression coefficients were fitted from World Ocean Atlas (WOA) data (Garcia et al., 2010) for subthermocline $\mathrm{NO_3}$ (restricting $z > 100\,\mathrm{m}$). Resulting values for a_N and b_N were 0.0074 and 10.85 for station India, and 0.018 and 3.91 for Biotrans. There were no obvious relationships between N_0 and depth for the two HNLC stations and so mean (fixed) values of 26.1 and 14.8 $\mathrm{mmol\,N\,m^{-3}}$ were used for N_0 for Kerfix and Papa respectively.

3.2 Ecosystem model description

The NPZD ecosystem model we have implemented in EMPOWER is presented in Fig. 4 with dissolved inorganic nitrogen (N; the sum of nitrate and ammonium), phytoplankton (P), zooplankton (Z) and detritus (D) as state variables. It is a simplification of the marine ecosystem inspired by that of FDM90 (note that, because we focus here on Station India, the version of the FDM90 model applied to Station India, Fasham (1993) provides the more pertinent foundation). Improved formulations are implemented for multiple-prey grazing, plankton mortality, regeneration and other detrital loss terms, as well as alterations to the parameterisation. The equations are described below; model parameterisation is described in Sect. 4.1. The phytoplankton equation is:

$$\frac{\mathrm{d}P}{\mathrm{d}t} = \mu_P P - G_P - m_P P - m_{P2} P^2 - \frac{\left(w_{\mathrm{mix}} + H'(t)\right) P}{H(t)} \tag{2}$$

where the terms are growth, grazing and non-grazing mortality (linear and quadratic), physical losses due to mixing across the bottom of the mixed layer, and dilution effects of entrainment. $H(t)$ is mixed layer depth (m) at time t and $H'(t)$ denotes the rate of change of H when $\mathrm{d}H/\mathrm{d}t$ is positive (dilution). As explained above, when $\mathrm{d}H/\mathrm{d}t$ is negative the change in density due to detrainment of mass from the mixed layer is exactly balanced by the increasing density due to decreases in volume, and therefore detrainment does not alter the concentration of remaining biomass. Variable μ_P is the vertically-averaged temperature-dependent daily growth rate, defined as the product of a temperature-dependent maximum growth rate, $\mu_P^{\max}(T)$, and non-dimensional limitation terms for nutrients and light, $L_N\ (N)$ and $L_I\ (I(t,z))$:

$$\mu_P = \mu_P^{\max}(T)L_N(N)L_I(I(t,z)) \tag{3}$$

Note that μ_P is calculated on a daily basis averaging over the time of day (t) and depth (z). Temperature and nutrients are assumed to be uniformly distributed throughout the mixed layer, in which case μ_P is:

$$\mu_P = \frac{\mu_P^{\max}(T)L_N(N)}{24H}\int_0^{24\,\mathrm{h}}\int_0^{H} L_I(I(t,z))\mathrm{d}z\mathrm{d}t \tag{4}$$

With the assumption of balanced growth, $\mu_P^{\max}(T)$ is equal to the equivalent maximum photosynthetic rate, $V_P^{\max}(T)$. The temperature dependence of photosynthesis is from Eppley (1972):

$$V_P^{\max}(T) = V_P^{\max}(0)1.066^T \tag{5}$$

where $V_P^{\max}(0)$ is photosynthesis at 0 °C. Note that this exponential relationship is equivalent to a Q_{10} of 1.895.

The traditional way NPZD-type models characterise nutrient limitation of phytoplankton growth rate by nutrients, $L_N(N)$, is calculated as a Michaelis–Menten (or Monod) relationship:

$$L_N(N) = \frac{N}{k_N + N} \tag{6}$$

where k_N is the half saturation constant.

The calculation of L_I is the most mathematically complicated aspect of characterising phytoplankton growth in this model as it takes into consideration both seasonal and diurnal patterns of irradiance arriving at the ocean surface (I_0), attenuation of irradiance with depth and photosynthesis as a function of light intensity. Light is assumed to vary with depth according to Beer's law ($I = I_0 \exp(-k_{\mathrm{PAR}} z)$) and photosynthesis calculated using a photosynthesis–irradiance (P–I) curve. The daily depth-average photosynthetic rate is calculated over the course of the day using an assumed daily variation of light, from which the daily average is derived. The user of EMPOWER is provided with a choice between two photosynthesis–irradiance (P–I) curves, a Smith function (Eq. 7) and an exponential function (Eq. 8) (Fig. 5):

$$V_P = \frac{\alpha I V_P^{\max}}{\sqrt{\left(V_P^{\max}\right)^2 + \alpha^2 I^2}} \tag{7}$$

$$V_P = V_P^{\max}\left(1 - \exp\left(-\alpha I / V_P^{\max}\right)\right) \tag{8}$$

Integration with depth (inner integral of Eq. 4) can be calculated analytically for either of the two P–I curves; equations are provided in Appendix B. The default method of handling the diurnal variation in irradiance at the ocean surface (outer integral of Eq. 4) is to do a numeric integration. The user may choose between assuming either a sinusoidal (Platt et al., 1990) or triangular (Steele, 1962; Evans and Parlsow, 1985) pattern of irradiance throughout each day, from sunrise to sunset and peaking at noon.

Analytic depth integrals require a Beer's law attenuation of light within the water column characterised by a single attenuation coefficient, k_{PAR}. The simplest assumption, provided as the first of two options in EMPOWER, is that k_{PAR} is the sum of attenuation due to water and phytoplankton, parameters k_w and k_c respectively:

$$k_{\mathrm{PAR}} = k_w + k_c P \tag{9}$$

Parameters k_w and k_c are often assigned values of 0.04 m^{-1} and 0.03 $\mathrm{m}^2\,(\mathrm{mmol\,N})^{-1}$ respectively (e.g., FDM90); these values are used in EMPOWER.

The assumption of a single mixed layer value of k_{PAR} is questionable because in reality the value of k_{PAR} varies with depth as a result of the changing spectral properties of the irradiance field. Red light is mostly absorbed by water in the upper few meters while blue penetrates deepest, with relatively efficient absorption by chlorophyll at both wavelengths. Based on a complex treatment of submarine light (Morel, 1988), a piecewise approach to light attenuation was developed by Anderson (1993) with different values, $k_{\mathrm{PAR},i}$, with $i = 1$ for depth range 0–5 m, $i = 2$ for depth range 5–23 m and $i = 3$ for depths > 23 m ($i = 1, 2, 3$), in each case k_{PAR} (i) is related to pigment (chlorophyll) concentration, C:

$$k_{\mathrm{PAR},i} = b_{0,i} + b_{1,i}C^{1/2} + b_{2,i}C + b_{3,i}C^{3/2} + b_{4,i}C^2 + b_{5,i}C^{5/2} \tag{10}$$

This approach to light attenuation is provided as the default option for use in EMPOWER. The values of the polynomial coefficients are listed in Table 2.

The diurnal variation in light at the ocean surface over the course of a day may be reasonably approximated by a sinusoidal function that is symmetric about noon irradiance (Platt, 1980). Further simplification is possible by use of a linear model, i.e., triangular centred at noon (e.g. Steele, 1962; Evans and Parlsow, 1985) because this simplifies the time integration. It should be noted here that despite Evans and Parslow's (1985) claim that differences between the triangular and sinusoidal approximations are minimal if the area under the curve is the same, they did not make the "equivalent area" adjustment to their formula, nor is their statement generically true (i.e. it depends on the peak light intensity, the attenuation of light with depth and the nonlinear P–I relationship).

In EMPOWER, the default method of handling the diurnal variation in irradiance at the ocean surface is to do a numeric integration. The user may choose between assuming either a sinusoidal (Platt et al., 1990) or triangular (Steele, 1962; Evans and Parlsow, 1985) pattern of irradiance throughout each day, from sunrise to sunset and peaking at noon. Undertaking a numerical time integral involves computational cost and two empirical methods (Evans and Parslow, 1985; Anderson, 1993) have been published that provide analytic calculations (i.e pre-determined formulae) for daily depth-integrated photosynthesis in a water column. Both are provided as options for use in EMPOWER and have the advantage of faster run time. The first of the two EMPOWER options is the depth-averaged light-dependent calculation of growth of Evans and Parslow (1985) which assumes a triangular pattern of daily irradiance, Beer's law for light attenuation (Eq. 9) and a Smith function as the *P*–*I* curve (Eq. 7). It has been a popular choice in previous slab modelling studies (Table 1). The second option is from Anderson (1993), which was developed as an empirical approximation to the spectrally resolved model of light attenuation and photosynthesis of Morel (1988) used in combination with the polynomial method of integrating daily photosynthesis of Platt et al. (1990). It assumes a sinusoidal pattern of irradiance through the day, a piecewise Beer's law light attenuation (Eq. 10) and an exponential function as the *P*–*I* curve (Eq. 8). Parameter α, the initial slope of the *P*–*I* curve, is also spectrally dependent. The method of Anderson (1993) calculates the variation of α with depth as a function of chlorophyll in the water column. Daily photosynthesis is then calculated using a polynomial approximation. The methods for calculating daily depth-integrated photosynthesis of Evans and Parslow (1985) and Anderson (1993) are non-trivial and, for completeness, the equations are supplied in Appendix C.

Grazing by zooplankton is assumed to be on both phytoplankton and detritus. This choice was made in part to illustrate how to implement ingestion on multiple prey types, as such functions are used for more complex models (e.g. when there are multiple phytoplankton size classes or functional types and/or omnivory by zooplankton). Many multiple-grazing formulations, however, comprise questionable assumptions about zooplantkon feeding behavior (Gentleman et al., 2003). For example, the multiple-prey grazing formula used in FDM90 and Fasham (1993) is classified as an active switching response (Gentleman et al., 2003) which can display anomalous behaviour such as sub-optimal feeding (i.e. ingestion rates decreasing when prey availability increases). We have therefore opted to improve upon Fasham's choice by using a different multiple-prey response, but one that is nevertheless commonplace in the literature. Specifically, we have adopted a passive switching response where density dependence of the prey preferences arises due to inherent differences in the single-prey responses (see Gentleman et al., 2003). This sigmoidal (or Holling Type 3) response characterised as (Fig. 6):

$$G_P = \left(\frac{I_{\max}\hat{\varphi}_P P}{k_Z^2 + \hat{\varphi}_P P + \hat{\varphi}_D D}\right) Z, \hat{\varphi}_P = \varphi_P P, \hat{\varphi} D = \varphi_D D \tag{11}$$

$$G_D = \left(\frac{I_{\max}\hat{\varphi}_D D}{k_Z^2 + \hat{\varphi}_P P + \hat{\varphi}_D D}\right) Z \tag{12}$$

where the term in parentheses is the zooplankton specific ingestion rate. This Sigmoidal formulation implies that the single-prey response for both phytoplankton and detritus are each sigmoidal (Type 3). Parameter $I_{\max}$ is the maximum specific grazing rate, which is the same for both phytoplankton and detritus and equates to their single prey maximum ingestion rates. Although parameters φ_P and φ_D are often called preferences in the literature, the actual prey preferences associated with this response (i.e. relative amount in the diet as compared to the environment) are density-dependent, with the relative preference for phytoplankton to detritus is determined by $\mathrm{pref}_{P:D} = \frac{\phi_P P}{\phi_D D} = \frac{\hat{\phi}_P}{\hat{\phi}_D}$. The φ parameters actually relate to the half-saturation constants associated with the single prey functional responses. Specifically, $\phi_P = \frac{k_Z^2}{k_P^2}$, where k_P is the half saturation value for the Type 3 single-prey response for ingestion of phytopalnkton, and φ_D is defined similarly. Parameter k_Z, which is often referred to as the half-saturation value in the literature, is actually an arbitrary parameter (i.e. this formulation is over-parameterized, see Gentleman et al., 2003) whose value determines the assumed single-prey half saturation constants based on choices for the φ parameters.

The Sigmoidal response assumes an interference effect of alternative prey in that as detritus increases, ingestion of phytoplankton decreases (with the same interaction for phytoplankton and ingestion of detritus). This interference effect is not so great as losing the benefit of generalism, i.e. total ingestion always increases for an increase in total prey density. The non-equal preferences reduce the interference effect for phytoplankton, i.e. the contours in the first panel of Fig. 6 are more vertical than for equal preferences. The corrollary effect is that the increased ingestion by consuming both phytoplankton and detritus vs. just phytoplankton is reduced as compared to when prey have equal preferences.

Regarding non-phytoplankton grazing mortality, Fasham (1993) used a non-linear Michaelis–Menten saturating function although a linear mortality term is the usual choice (e.g., FDM90). We opted for the more flexible approach of using both linear and nonlinear terms (Yool et al., 2011, 2013a). The former may account for metabolic losses or natural mortality. The use of an additional nonlinear term represents density-dependent loss processes, notably mortality due to infection by viruses. The abundance of viruses is highly dependent on the density of potential host cells (e.g., Weinbauer, 2004) and, as reviewed by Danovaro et al. (2011), there is “compelling” evidence that, at least in some instances, viruses are responsible for the demise of phytoplankton blooms based on observations of high proportions (10–50 %) of infected cells (e.g., Bratbak et al., 1993, 1996). A quadratic form was used for the nonlinear mortality term (e.g., Kawamiya et al., 1995; Oschlies and Schartau, 2005) and all phytoplankton non-grazing mortality losses were allocated to detritus.

The equation for rate of change of zooplankton density is:

$$\frac{\mathrm{d}Z}{\mathrm{d}t} = (\beta k_N(G_P + G_D)) - \left(m_Z Z + m_{Z2} Z^2\right) - \frac{\left(w_{\mathrm{mix}} + H'(t)\right) Z}{H(t)} \qquad (13)$$

where the terms are growth, mortality (linear and quadratic) and losses due to mixing and changing MLD. Zooplankton growth can be described as the product of gross growth efficiency (GGE) and intake, where GGEs are typically between 0.2 and 0.3 (Straile, 1997). Gross growth efficiency is itself the product of absorption efficiency, β (more commonly, but incorrectly, known as assimilation efficiency; e.g. see Mayor et al., 2011) and net production efficiency, k_{NZ}. Splitting into these separate parameters permits three-way fractionation of intake between egestion (i.e. faecal pellet production, $1-\beta$), growth ($\beta \cdot k_{NZ} = \text{GGE}$; first term in Eq. 13) and excretion ($\beta(1-k_{NZ})$).

A variety of formulations exist in ecosystem models to describe zooplankton mortality and the appropriate functional form has been and continues to be a hotly debated topic (Steele and Henderson, 1992; Edwards and Yool, 2000; Mitra et al., 2014). Most common are the linear and quadratic terms, although some authors have chosen to employ other non-linear functions (e.g. Fasham, 1993 used a Michaelis–Menten relationship). As with phytoplankton, we used both linear and quadratic non-linear terms (Yool et al., 2011). The linear term represents density-independent natural mortality, whereas the quadratic term is considered to be due to predation by carnivores (whose population tracks that of the zooplankton). The different sources of mortality result in different fates for these terms. Loss from natural mortality is allocated to modelled detritus, which implies a broader size-class of modeled particulates (and therefore higher sinking rates) than when just phytoplankton death contributes to this variable.

The fate of the predation-related mortality is less obvious because the metabolic activity of higher predators would result in ingested material being converted into dissolved nutrients as well as larger particulates (e.g. fecal pellets and death). Moreover, the higher predators may export material from the local region with migration. FDM90, along with a suite of follow-on models, therefore chose to allocate predation-related zooplankton mortality between nutrients (ammonium and DON, attributed to excretion by higher predators) and material that is immediately exported from the system (e.g. attributed to fast-sinking detritus generated by higher predators). Similarly, Steele and Henderson (1992) also allocated zooplankton mortality to export. Nevertheless, many past and recent published marine ecosystem modelling studies allocate all of zooplankton mortality to detritus (Oschlies and Schartau, 2005; Salihoglu et al., 2008; Hinckley et al., 2009; Ye et al., 2012). We argue, however, that this is not necessarily realistic given that detrital particles related to higher-predators are larger and therefore even faster-sinking than that produced by the modelled plankton. We have therefore here adopted to follow the sage approach of the model pioneers and assume that the predation-related mortality represented by our quadratic term is instantly exported and thereby entirely lost from the surface mixed layer of the model. As with phytoplankton, zooplankton are subject to changes in concentration via mixing and changes in MLD.

The equation for the rate of change of dissolved inorganic nitrogen (DIN) density is:

$$\frac{\mathrm{d}N}{\mathrm{d}t} = -\mu_P P + \beta(1 - k_{\mathrm{NZ}})(G_P + G_D) + m_D D + \frac{\left(w_{\mathrm{mix}} + H'(t)\right)(N_0 - N)}{H} \tag{14}$$

DIN is taken up by phytoplankton (first term) and, via the food web, regenerated with terms 2 and 3 in Eq. (14) representing excretion by zooplankton and remineralisation of detritus respectively. The fourth term represents the net transport due to mixing (i.e. supply by the deep water and loss from the surface layer). The last term represents the net effect of volume changes, i.e. increases in DIN density due to supply of deep water nutrients through entrainment and decreases in DIN density due to volume increases associated with entrainment.

Finally, the detritus equation is:

$$\begin{aligned}\frac{\mathrm{d}D}{\mathrm{d}t} &= m_P P + m_{P2} P^2 + m_Z Z + (1 - \beta)(G_P + G_D) - G_D \\ &\quad - m_D D - \frac{\left(w_{\mathrm{mix}} + H'(t) + v_D\right) D}{H}\end{aligned} \tag{15}$$

Detritus is produced by phytoplankton mortality, zooplankton natural mortality (linear term) and as zooplankton egestion (faecal pellet production). It is lost by zooplankton grazing and is also remineralised at a constant rate, m_D. Detritus is mixed and subject to changes via the seasonal cycle of MLD in the same manner as phytoplankton and zooplankton (terms 6 and 7), and also experiences losses due to gravitational sinking (last term). This occurs at rate v_D ($\mathrm{m\,d^{-1}}$) and provides direct export of particulate organic matter to the layer below (where it is implicitly remineralised back to DIN).

The first results Sects. 4.1 and 4.2 are devoted to parameterising the model for station India and a detailed description of values assigned to model parameters is provided therein.

3.3 Setup in R

We have chosen to code our model in the R programming language which can be readily downloaded for free over the internet. Input and output files are in ASCII text (.txt) format, avoiding the use of proprietary software. The structure of the code is designed to be transparent, where possible using conventional syntax common to different programming languages such as the use of loops, block IF statements, etc. As such, it can be relatively easily altered or translated into another programming language, if need be. Where possible, we have followed what we consider to be best practice in developing the code which includes:

i. Creation of a fixed segment of core code that handles the numerical integration, as well as writing to output files. Being fixed, this segment does not require alteration in the event of changes to the ecosystem model formulation, nor indeed if an entirely new ecosystem model is implemented.

ii. The ecosystem model formulation, i.e., the specification of the terms in the differential equations and calculation of their rates of change, is handled by a function (FNget_flux) that is external to the core code.

iii. The specification of parameter values and run characteristics (e.g., time step, run duration, as well as flags for choices between different formats for export to output files, choice of ocean location and for different parameterisations of key processes) is via text files that are read in at the onset of each simulation. Thus, there is no need to enter or alter the model code when changing parameter values or other model settings.

iv. When a model run finishes, the summed annual fluxes associated with each term in the differential equations is displayed on the computer screen along with a report as to whether mass balance is achieved for each state variable (over the last year of simulation). Basic checking of mass balance is useful for ensuring that the model equations are error-free.

v. Regimented layout for clarity with extensive commenting throughout.

The R programming language is supported by various libraries that can be accessed via the internet. One such library is for solving ordinary differential equations (Soetaert et al., 2010). Using this library has the advantage of minimising the length of the code and offers flexibility in terms of a range of numerical methods. On the other hand, its implementation requires that various conventions are adhered to and these can be restrictive when it comes to producing ancillary code, e.g., the formatting and export of output files. As such, we opted to code the numerical solution of the ODEs manually within the core code of the model for several reasons:

i. It offers full transparency for the interested user who wishes to see the method of integration.

ii. The use of manual code makes it considerably easier to export chosen variables and fluxes to output files in desired formats and frequencies.

iii. In our case, the user is given the choice between two integration methods, Euler and fourth order Runge Kutta (RK4). These methods, particularly the latter, are entirely sufficient for the numerical task at hand and the coding of them is straightforward.

iv. By using elementary syntax, the code can be easily altered or converted to other programming languages.

v. The code is stand alone and not subject to reformulation in the event of future changes in subroutine libraries.

The structure of the code is shown in Fig. 7. The functions come first, appearing prior to the core code in R. The key function call is FNget_flux which contains the ecosystem model specification. The rate of change is calculated for each term in the differential equations and allocated to a 2-D array (flux no., state variable no.) which is then passed back to the core (permanent) code for processing. Other functions are: FNdaylcalc (calculates length of day), FNnoonparcalc (noon irradiance, PAR), FNLIcalcNum (undertakes numerical (over time) calculation of daily depth-integrated photosynthesis), FNLIcalcEP85 (calculates L_I using the equations of Evans and Parslow, 1985), FNaphy (calculates chlorophyll absorption, effectively parameter α, in the water column after Anderson, 1993) and FNLIcalcA93 (calculates L_I using the equations of Anderson, 1993).

Model setup comes next. Parameter values are read in from file NPZD_parms.txt. Simulation characteristics are then read in from file NPZDextra.txt. These include:

i. Initial values for state variables.

ii. Run duration (years) and time step.

iii. Choice of station: India, Biotrans, Papa, Kerfix.

iv. Choice of photosynthesis calculation: numeric (default), Evans and Parslow (1985) or Anderson (1993).

v. Choice of integration method: Euler or RK4.

vi. Choice of output characteristics: none, last year only or whole simulation, and a frequency of once per day or every time step.

Model forcing for the chosen station of interest is then assigned. Monthly values of MLD and SST are read in and subject to linear interpolation in order to derive daily forcing. Other forcing variables are also set: latitude, deep nitrate (N_0; Eq. 1) and cloud fraction. At the end of the setup section there are a few lines of code that need to be altered if the ecosystem model is changed. These lines tell the computer how many state variables the model has, the maximum number of flux terms associated with any one state variable and the maximum number of auxiliary variables to be stored for writing to output files.

An advantage of this structure is that an initial section of customisable code is followed by a section of permanent code that does not require adjustment in the event of changes to the equations that describe the ecosystem model, or indeed if a completely new ecosystem model is to be used. This code sets up a series of matrices to store fluxes and outputs and then integrates the model equations over time. State variables are updated and results exported to three output files: out_statevars.txt (state variables), out_aux.txt (chosen auxiliary variables) and out_fluxes.txt (all the terms in the differential equations). These text files are readily imported to, for example, Microsoft Excel.

Results are plotted graphically on the computer screen at the completion of each simulation run. The graph plotting code is necessarily model specific and needs to be updated by the user as required. R is a user friendly programming language in this regard and the code provided should be sufficient for the user to incorporate extra variables with ease.

Finally, a user guide is provided in Appendix D, outlining how to set up R, run the code, a summary of input and output files, and guidance on considerations when altering the ecosystem code and/or forcing.

Title Page
Abstract | Introduction
Conclusions | References
Tables | Figures
◀◀ | ▶▶
◀ | ▶
Back | Close
Full Screen / Esc
Printer-friendly Version
Interactive Discussion

4 Results

Model results are presented in four sections. First, a simulation is shown for station India using parameters taken from the literature (Sect. 4.1). Parameter tuning is then undertaken to fit all four ocean time series stations, India, Biotrans, Papa and Kerfix, to data for chlorophyll and nitrate at each site (Sect. 4.2). Moving on from the calibration of parameters, structural sensitivity analysis is then carried out by examining model sensitivity to equations for the calculation of daily depth-integrated photosynthesis (Sect. 4.3) and mortality of phytoplankton and zooplankton (Sect. 4.4).

4.1 Parameter initialisation: station India

Adjustment of parameters is a perennial problem for modellers. Parameters can be set from the literature, sometimes directly on the basis of observation and experiment, but the usual starting point is to take values from previously published modelling studies. Almost inevitably, however, the resulting simulations will show mismatch with data and parameters are usually selected for adjustment (tuning) to improve the agreement with data. One option is to use objective tuning methods, such as the genetic algorithm or adjoint method in which many or all of the model parameters are varied simultaneously in order to try and find a best fit solution to data (e.g., Friedrichs et al., 2007; Record et al., 2010; Ward et al., 2010; Xiao and Friedrichs, 2014). The advantage is objectivity, but difficulties include sloppy parameter sensitivities (parameters compensate for each other), different values of model parameters may be similarly consistent with the data (the problem of identifiability), exploration of a huge parameter space may be required and local minima in misfit parameter space can make it difficult to find the true global minimum (Slezak et al., 2010). It is usually the case that models are underdetermined by data anyway (Ward et al., 2010), i.e., there are insufficient data (in terms of absolute amount and/or different types of data) to adequately constrain parameter values. And of course, objective methods require expertise, time and computing resources.

Modellers more often than not carry out parameter adjustment by varying values of chosen parameters one at a time until satisfactory convergence with data is achieved. The skill is in deciding which parameters to vary. In principle, sensitivity analysis can be of help in this regard in that sensitive parameters can be identified and selected for adjustment if they can be justifiably altered (i.e., there is uncertainty regarding their value). Here, we will demonstrate the use of EMPOWER for model calibration. Parameter sets will be derived for the four stations, India and Biotrans in the North Atlantic and the HNLC stations Papa (subarctic North Pacific) and Kerfix (Southern Ocean). The NPZD model we have presented is a new one and, as such, there is no readily available complete set of parameter values to draw upon. Using our experience, we chose appropriate parameter values from the literature and adjusted others to give a good fit with the data for station India. This result is presented below along with a discussion of how we went about achieving this parameter set. Working from this parameter set, tuning of parameters is then undertaken to fit the other stations to the data.

Station India was previously modelled by Fasham (1993) and we used this publication as a starting point for the assignment of parameter values. Those parameters that differed from Fasham (1993) were otherwise parameterised from the literature where possible and/or selected as a best guess. The resulting parameter set, along with adjusted values (see below), is shown in Table 3.

The maximum phytoplankton growth rate used by Fasham (1993) for station India was 1.25 d^{-1}. The equivalent parameter in our model is the maximum rate of photosynthesis, $V_P^{\max}$, which is usually expressed in units of $\mathrm{g\,C\,(g\,Chl)^{-1}\,h^{-1}}$, requiring unit conversion. The Redfield C : N molar ratio of 6.625 is the obvious choice to convert between C and N. Carbon to chlorophyll ratios are more variable and a value of 50 $\mathrm{g\,C\,(g\,Chl)^{-1}}$ has previously been used in modelling studies (e.g., Fasham et al., 1990). However, C : Chl ratios are known to vary widely in response to ambient conditions. The recent study of Sathyendranath et al. (2009) found the North Atlantic ratio to typically vary between 50 and 100 $\mathrm{g\,C\,(g\,Chl)^{-1}}$, so here we use an intermediate value of 75 $\mathrm{g\,C\,(g\,Chl)^{-1}}$ (parameter θ_{chl}). Converting units, $V_P^{\max}$ of 1.25 d^{-1} is equivalent to 3.9 g C (g Chl)$^{-1}$ h^{-1} which is within a range of typical values for V_P at ambient temperatures ranging between 1 and 5 g C (g Chl)$^{-1}$ h^{-1} (e.g., Harrison and Platt, 1986; Cullen, 1990; Platt et al., 1990; Rey, 1991). We include temperature-dependence of this parameter and so, assuming that the rate of 3.9 d^{-1} occurs at a typical sea surface temperature during the bloom for station India of 10 °C, $V_P^{\max}(0)$ is then 2.0 d^{-1} (Eq. 4). Using the same conversion of units, Fasham's (1993) value for parameter α of 0.025 (W m^{-2})$^{-1}$ d^{-1} converts to 0.08 g C (g Chl)$^{-1}$ h^{-1} (W m^{-2})$^{-1}$. Remaining phytoplankton parameters are k_N, 0.5 mmol N m^{-3} (Fasham, 1993), m_P, 0.02 d^{-1} (Yool et al., 2011, 2013a), and m_{P2}, 0.025 (mmol N m^{-3})$^{-1}$ d^{-1} (Oschlies and Garçon, 2005).

Zooplankton parameters $I_{\max}$ and k_Z were assigned directly from Fasham (1993) with values of 1.0 d^{-1} and 1.0 mmol N m^{-3}, respectively. Note that assimilation efficiency as used by Fasham (1993) is in fact a growth efficiency whereas our use of absorption efficiency (parameter β) is more in keeping with contemporary zooplankton modelling (e.g., see Anderson et al., 2013) and refers to the fraction of material absorbed across the gut and is multiplied by a net production efficiency (parameter k_{NZ}) to give growth efficiency. Values of 0.69 and 0.75 were assigned to parameters β and k_{NZ} respectively (Anderson, 1994; Anderson and Hessen, 1995). In the model of Fasham (1993), zooplankton grazed on phytoplankton, bacteria and detritus. The model here has no bacteria and the relative ratio of grazing preferences for phytoplankton and detritus was maintained by assigning values for φ_P and φ_D of 0.67 and 0.33 respectively, i.e. a 2 fold difference. Thus when we set $k_Z = 1$ mmol N m^{-3}, this implies that the phytoplankton single-prey half-saturation is 1.22 mmol N m^{-3} and the detritus single-prey half-saturation constant is 1.75 mmol N m^{-3}. The implied single-prey half-saturation constants change to 0.64 and 0.91 respectively when $k_Z = 0.52$ mmol N m^{-3}. Mortality parameters m_Z and m_{Z2} were assigned values of 0.02 d^{-1} (Yool et al., 2011, 2013a) and 0.34 (mmol N m^{-3})$^{-1}$ d^{-1} (Oschlies and Schartau, 2005), respectively.

A detritus sinking rate of 1.0 m d^{-1} was used by Fasham (1993), a value at the low end of that typically used in models. Detritus is in reality composed of a range of sinking material including faecal pellets and marine snow with sinking speeds of between 5 and 100s $\mathrm{m\,d^{-1}}$ (Wilson et al., 2008), as well as slow-sinking material that is likely to be remineralised in the upper water column (Riley et al., 2012). A typical sinking rate used in ecosystem models is between 5 and 10 $\mathrm{m\,d^{-1}}$ (e.g, Fasham et al., 1990; Oschlies et al., 1999; Anderson and Pondaven, 2003; Llebot et al., 2010; Kidson et al., 2013). We used a value for V_D of 5.0 $\mathrm{m\,d^{-1}}$, noting that results differed only slightly compared to using a sinking rate of 1.0 $\mathrm{m\,d^{-1}}$. Note also that the detritus produced by quadratic zooplankton mortality is assumed to be very fast sinking and is instantly exported from the upper mixed layer. The remineralisation rate of detritus (parameter m_D) was set to 0.05 $\mathrm{d^{-1}}$ (Fasham, 1993). Finally, parameter w_{mix} was set to 0.1 $\mathrm{m\,d^{-1}}$ (Fasham et al., 1990).

Choices have to be made regarding the settings for calculating daily depth-integrated photosynthesis. A sinusoidal pattern of daily irradiance was set as default for this purpose, with a numeric integration over time of day. A Smith function was chosen as the P–I curve (Eq. 7) permitting a straightforward analytic depth integral for photosynthesis (Appendix B). Photosynthesis at depth can be vertically integrated analytically, when light extinction in the water column is described by Beer's law with a constant coefficient. As default, we use the piecewise Beer's law treatment of Anderson (1993) in which the water column is divided into three depth zones (0–5, 5–23 and > 23 m) and a separate extinction coefficient calculated for each as a function of chlorophyll (Eq. 10). Although this approach is more complicated that using a single extinction coefficient, it is easily justified a priori given the improved representation of light attenuation and its impact on predicted primary production (Anderson, 1993). Model sensitivity to these various assumptions regarding the calculation of light attenuation and photosynthesis will be examined in Sect. 4.3, including an assessment of the performance of the algorithms of Evans and Parslow (1985) and Anderson (1993).

The model was run for three years, by which time it generates a repeating annual cycle of plankton dynamics. The chlorophyll data are SeaWiFS 8 day averages (O'Reilly et al., 1998). We had access to data from 1998 to 2013. Averaging data across years to provide a climatological seasonal cycle of chlorophyll is not useful because key features, such as the spring phytoplankton bloom, are smoothed out because the bloom timing is variable between years. A characteristic year was therefore chosen, in this case 2006, with which to compare the model to data. Nitrate data are from World Ocean Atlas (Garcia et al., 2010). The last year of simulation is compared to data for chlorophyll and nitrate in Fig. 8. Nitrate (model DIN) is remarkably well predicted using these default parameter settings. Model chlorophyll shows a less good match with data. The timing of the spring bloom is too late although this could, at least in part, be due to the MLD forcing which was climatological, rather than for year 2006 (the chlorophyll data). Predicted chlorophyll also appears to be too high during the spring and summer period. Parameter adjustment is therefore desirable in order to improve the fit with data.

4.2 Model calibration

Many modelers go about parameter adjustment on a trial-and-error basis, making ad hoc changes to parameters and observing the outcome. A more structured way of going about this is to undertake a systematic sensitivity analysis of parameters and then, informed by this analysis, choose which parameters to vary. We use EMPOWER to demonstrate this practice here. Three variables were selected as simple measures of model mismatch with data: minimum DIN encountered during the seasonal cycle, N_{min}, which is a logical choice because it is desirable to correctly predict DIN drawdown during the spring period, maximum chlorophyll at the peak of the spring bloom, $\mathrm{chl}_{\mathrm{max}}$ and the average summer chlorophyll between days 200 and 300, $\mathrm{chl}_{\mathrm{av}}$. Values of these three quantities, as outputs from the run shown in Fig. 8, were 1.49 $\mathrm{mmol\,N\,m^{-3}}$ for N_{min} and 3.34 and 0.59 $\mathrm{mg\,Chl\,m^{-3}}$ for $\mathrm{chl}_{\mathrm{max}}$ and $\mathrm{chl}_{\mathrm{av}}$ respectively. Model parameters were varied ±10 % and the change in these variables quantified in terms of normalised sensitivity:

$$S(p) = \frac{(W(p) - W_{\mathrm{S}})/W_{\mathrm{S}}}{(p - p_{\mathrm{S}})/p_{\mathrm{S}}} \tag{16}$$

where W_S is the value of a given variable (in this case N_{min}, chl_{max} or chl_{av}) for the standard parameter set with parameter value p_S, and $W(p)$ is the value when the parameter is given value p. Results are shown in Table 4, ordered high to low for sensitivity of chl_{av}.

The chlorophyll data are too few in number to reliably infer the magnitude of the spring bloom whereas there are many data points providing an average chlorophyll between days 200 and 300 of 0.29 mg m^{-3}. Looking at Table 4, chl_{av} is sensitive to grazing parameters, notably k_Z. As the first step to improving the model fit to data, k_Z was decreased until predicted chl_{av} was equal to 0.29 mg m^{-3}, resulting in a decrease in the value of this parameter from 1.0 to 0.52 mmol N m^{-3}. Separate values for parameter k_Z of 0.8 and 0.3 mmol N m^{-3} were used for micro and mesozooplankton in the model of Yool et al. (2011, 2013a). Values for k_Z lower than 1.0 mmol N m^{-3} have also been used in other models, e.g., values of 0.75 and 0.8 mmol N m^{-3} were used by Anderson and Pondaven (2003) and Llebot et al. (2010) respectively. Decreasing k_Z to 0.52 mmol N m^{-3} led to a change in predicted N_{min} from 1.49 to 4.92 mmol N m^{-3}. The required N_{min} is about 3.0 mmol N m^{-3} and in order to redress this mismatch with data parameter α was chosen for adjustment. This parameter shows high sensitivity for N_{min} and relatively low sensitivity for chl_{av} and chl_{max}. Intuitively, α is a logical parameter to choose because nitrate drawdown occurs during rapid growth of phytoplankton at the onset of the spring bloom and increasing this parameter will therefore enhance drawdown. An increase in α is also easily justified based on observational data (e.g., Rey et al., 1991). Increasing the value of α from 0.08 to 0.12 g C (g Chl)$^{-1}$ h^{-1} (W m^{-2})$^{-1}$ gave a predicted N_{min} of 2.82 mmol N m^{-3} and an overall good fit to the data (Fig. 9). The only obvious mismatch is in the overwinter chlorophyll but extremely low values are a common feature of slab-type models. The mismatch can be improved by removing the linear phytoplankton mortality (see Sect. 4.4, and discussion therein). A further consideration is that phytoplankton may adjust their C : Chl ratio in winter to mitigate the effect of the low light intensities that they experience. We consider removing this mortality term unrealistic. It is no good getting the right result for the wrong reasons and so chose to keep phytoplankton mortality as it is. There is also a hint that the timing of the bloom is a little late but, bearing in mind we used climatological cycle of annual mixed layer depth and light, whereas the data are for a single year, 2006, this is not particularly surprising.

The associated seasonal cycles of P, Z and D, along with primary production, phytoplankton grazing and mortality are shown in Fig. 10. The peak of Z lags seven days behind that of P, illustrating the decoupling of phytoplankton and zooplankton during the spring bloom period. Primary production remains relatively high over summer, tightly coupled to grazing, sufficient to keep phytoplankton biomass in check. It might be expected that Station Biotrans is simulated accurately with the same parameter values as those of Station India because of their relatively close proximity in the northern North Atlantic Ocean and this is indeed the case (Fig. 11).

The two HNLC stations can be expected to require alternative parameterisations to the two North Atlantic stations because the food web structure differs between the two types of system. In contrast to the diatom spring bloom in the northern North Atlantic, iron-limited HNLC systems favour small phytoplankton which are tightly coupled to microzooplankton grazers (Landry et al., 1997, 2011), "grazer controlled phytoplankton populations in an iron-limited ecosystem" (Price et al., 1994). Simulations for stations Papa, showing both the unfitted and fitted model, are shown below in in Fig. 12. The unfitted model solution corresponds to parameters as for the best-fit solution to Station India (Table 3). In common with the data, there is no predicted chlorophyll bloom. Predicted chlorophyll is however on the upper bound of the data and predicted drawdown of nitrate is too severe, suggesting that the modelled phytoplankton growth rate is too high. Low growth rate of phytoplankton may be expected relative to the North Atlantic because of iron limitation and so parameter $V_P^{\max}(0)$, acting as a proxy for iron limitation, was halved in value to $1.0\,\mathrm{g\,C\,(g\,Chl)^{-1}\,h^{-1}}$. With this parameter setting, the model does a remarkably good job at reproducing the data, without need for further parameter adjustment.

A similar exercise was carried out for station Kerfix. Using the same parameter set as for station Papa, predicted chlorophyll was too high during the austral summer (Fig. 13). If grazing is dominated by microzooplankton, maximum grazing rate (parameter I_{max}) may be as high as 2.0 d^{-1} (Mongin et al., 2006). On this basis, I_{max} was increased until predicted chl_{max} (the maximum chlorophyll) equalled 0.35. A reasonable fit to the data was achieved with I_{max} equal to 1.4 d^{-1}.

4.3 Sensitivity to photosynthesis algorithm

Structural sensitivity analysis is performed to assess model sensitivity to the different assumptions for calculating daily depth-integrated photosynthesis. The best-fit simulation for Station India presented above (Fig. 9) is used as the baseline for comparison. Default settings in the baseline simulation were a numerical time integration (over the day), a Smith function for the *P–I* curve, and a sinusoidal pattern of daily irradiance and the piecewise application of Beer's law (Eq. 10; Anderson, 1993) for light attenuation in the water column.

The first sensitivity test involved changing the *P–I* curve from a Smith function (Eq. 7) to an exponential function (Eq. 8). Predicted seasonal cycles for chlorophyll and nitrate at station India are shown in Fig. 14. Results changed little with respect to the baseline simulation, with nitrate drawdown being slightly less when using the exponential *P–I* curve. Predicted chlorophyll was barely distinguishable between the two simulations. It is perhaps unsurprising that the model shows minimal sensitivity to choice of *P–I* curve as the shapes of the two curves are similar. Slightly higher photosynthesis is predicted using the Smith function for mid-range irradiance (Fig. 5), consistent with higher drawdown of NO_3. In a similar study by Anderson et al. (2010), however, remarkable sensitivity was seen to choice of the exact form of the zooplankton functional response. Other studies have also shown "alarming" sensitivity to apparently small changes in the specification of biological models (e.g. Wood and Thomas, 1999; Fussmann and Blasius, 2005).

Reverting to the Smith function as the chosen *P–I* curve, model predictions were next compared for simulations using sinusoidal vs. triangular irradiance (Fig. 15). Once again, the difference between the two simulations is relatively minor, although predicted drawdown of nutrient was about 2 $\mathrm{mmol\,m^{-3}}$ less when using the triangular assumption. The triangular approximation underestimates the period of high light relative to sinusoidal, for equivalent noon irradiance, with lower growth rate and associated drawdown of nutrient. It is worth noting, however, that the sensitivity shown here is at least as great as that for the choice of *P–I* curve, but has generally received much less attention in the literature.

Model sensitivity of predicted primary production to the equations describing light attenuation in the water column was previously highlighted by Anderson (1993), although without extending to analysis using full ecosystem models. A marked difference was seen here when the piecewise Beer's law for calculating light attenuation (Eq. 10) was replaced with a simple Beer's law (Eq. 9) (Fig. 16). The difference between the simulations can be understood by comparing k_{PAR} as a function of phytoplankton concentration for the two algorithms (Fig. 17). The single Beer's law of Eq. (9) predicts a modest increase in k_{PAR} from 0.04 $\mathrm{m^{-1}}$ at zero phytoplankton to 0.1 $\mathrm{m^{-1}}$ at $P = 1\,\mathrm{mmol\,N\,m^{-3}}$. The main difference with the piecewise Beer's law is the much greater light extinction in the upper 5 m of the water column, with k_{PAR} of 0.13 $\mathrm{m^{-1}}$ at $P = 0\,\mathrm{mmol\,N\,m^{-3}}$, increasing to 0.23 $\mathrm{m^{-1}}$ at $P = 1\,\mathrm{mmol\,N\,m^{-3}}$. A lesser rate of light attenuation using the simple Beer's law leads to greater penetration of light into the water column. The resulting higher photosynthesis over winter produced a larger spring bloom of phytoplankton and greater predicted drawdown of $\mathrm{NO_3}$. It is worth noting that the model sensitivity to this choice of light attenuation algorithm (both in terms of overestimating the spring bloom and the nutrient drawdown) is greater than that associated with the original parameter adjustment exercise for station India, highlighting the importance of carefully selecting formulations for key processes prior to parameter tuning.

Finally, there is the option to use the routines of Evans and Parslow (1985) and Anderson (1993) to calculate daily-depth integrated photosynthesis, without recourse to using numerical integration over time. Evans and Parslow used a Smith function for photosynthesis in combination with a triangular pattern of daily irradiance. This corresponds exactly to the simulation in Fig. 15 above for triangular irradiance. Thus, running the model using the Evans and Parslow equations (Appendix C) produces a result indistinguishable from the numerical simulation. Matters are not so simple when using the Anderson (1993) equations to calculate daily depth-integrated photosynthesis. The assumptions here are an exponential *P–I* curve and sinusoidal light, corresponding to the exponential *P–I* curve simulation in Fig. 14. But there is the additional assumption that parameter α, in addition to k_{PAR}, is spectrally dependent and varies in the water column. Thus, running the model with both light attenuation and photosynthesis calculated as in Anderson (1993) gives rise to a different simulation (Fig. 18). It is noticeable that, when using the A93 method, primary production is higher over winter, a result of elevated α, giving rise to an earlier spring chlorophyll bloom and greater drawdown of nitrate. Nevertheless, the simulation is entirely credible and we can recommend the use of the Anderson (1993) for use in marine ecosystem models.

4.4 Mortality terms

The model includes two mortality terms, linear and quadratic, for each of phytoplankton and zooplankton. This approach has previously been used in other models (e.g., Yool et al., 2011, 2013a), giving maximum flexibility. The obvious question is whether all four terms are actually needed. As a simple structural sensitivity analysis, we removed each of the four mortality terms in turn and show the impact on the predicted seasonal cycles of chlorophyll and nitrate, for Station India. Starting with the phytoplankton terms, setting m_P or m_{P2} to zero affected both the predicted timing and magnitude of the spring bloom (Fig. 19). One can argue that, although the predicted magnitude of the spring bloom looks a little low, removal of the linear term (setting $m_P = 0$) improved the model fit for chlorophyll, notably over winter. It seems hard to justify that loss rates should go to near zero at low population densities (the consequence of using a quadratic term only) because all organisms have metabolic requirements. Nearly all marine ecosystem models do, therefore, include a linear term for phytoplankton mortality and, for our baseline simulation (Sect. 4.2), we chose to keep this term on a purely conceptual basis. Given deep mixing, it is surprising that phytoplankton biomass, as seen in the data, is maintained over winter in high latitude waters. The reasons why this is so remain a matter of conjecture with candidate theories including cyclic motion associated with convective mixing (Huisman et al., 2002; Backhaus et al., 2003), and phytoplankton motility or buoyancy to remain near the ocean surface (see Ward and Waniek, 2007, and references therein). The slab model, and indeed 1-D and 3-D models, have difficulty dealing with this issue but there is no evidence that this seriously compromises results when it comes to the predicted timing and magnitude of the spring bloom and associated ecosystem dynamics later in the year. In contrast to the representation of linear mortality, many models do not include a non-linear phytoplankton mortality term but it seemed to perform well here. When it was removed, the predicted phytoplankton spring bloom was rather too high.

Results show that non-grazing phytoplankton mortality had a pronounced influence on simulated phytoplankton biomass both prior to and during the initiation of spring bloom (Fig. 19). It is at this time of year correspond when grazing losses are minimal (Fig. 10) such that phytoplankton dynamics are driven by the balance of growth and non-grazing mortality. Phytoplankton levels are low at the end of winter and hence removal of the quadratic mortality term had virtually no effect on pre-bloom phytoplankton levels whereas removal of the linear term had a marked impact leading to a reduction in the peak of the bloom of about a third. This reduction can be explained by the fact that the higher phytoplankton density pre-bloom associated with removal of linear phytoplankton mortality enabled higher pre-bloom zooplankton grazing. In contrast, removal of the quadratic mortality term nearly doubled size of the bloom, as might be expected based on the sensitivity analysis (Table 4). This strong effect on biomass indicates that it was the density-dependent (quadratic) mortality term that caused phytoplankton mortality to initially rival grazing (Fig. 10).

Removing the zooplankton mortality terms in turn also significantly impacted on model predictions (Fig. 20). While changes in the linear mortality term had a noteworthy effect on both the bloom peak and minimum drawdown (as also shown in the sensitivity analysis Table 4), it was the quadratic zooplankton mortality term that had the most influence. Removal of quadratic mortality resulted in significantly lower phytoplankton levels post-bloom (Fig. 20, Table 4) which is unsurprising since more zooplankton means more grazing. Perhaps less obvious is the result that removal of quadratic closure resulted in large changes in predicted post-bloom nitrate levels, even exceeding those arising from consideration of piecewise vs. simple light attenuation (Fig. 16). Predation-related losses, the quadratic term, were assumed to be instantly exported and thereby lost from the surface mixed layer of the model. Thus, when these losses are set to zero (parameter $m_{Z2} = 0$), nitrate drawdown is significantly diminished because, instead of being instantly exported, zooplankton quadratic mortality is allocated to sinking detritus, part of which is remineralised in the mixed layer. Overall, the work highlights the need for careful consideration of the parameterisation of closure in models, including the fate of material thereof.

5 Discussion

Simple models are all too often brushed aside in marine science today. When it comes to the representation of the marine ecosystem, complex models have come to the fore that have, for example, any number of plankton functional types, multiple nutrients, dissolved organic matter and bacteria, etc. (e.g., Blackford et al., 2004; Moore et al., 2004; Le Quere et al., 2005). There is a similar trend with ocean physics toward large, computationally demanding models. Many publications in recent years have involved the use of 3-D models (e.g., Le Quéré et al., 2005; Wiggert et al., 2006; Follows et al., 2007; Hashioka et al., 2013; Yool et al., 2013b; Vallina et al., 2014), although 1-D models are also well represented (e.g., Vallina et al., 2008; Kearney et al., 2012; Ward et al., 2013). Of course, the improved realism that is gained by using complex models is in general to be welcomed, with the caveat that improvements in prediction can only be achieved if the processes of interest can be adequately parameterised (Anderson, 2005).

Despite the trend to complex ecosystem models embedded in advanced physical frameworks, there nevertheless remains a place today, we argue, for simple models. Simple models are fast to run, transparent and easy to analyse. Marine ecosystem modelling can be somewhat of a black art in deciding what to include in terms of state variables, which formulations to apply for key processes such as photosynthesis, grazing and mortality, and in finding suitable parameter values. Simple models allow us to fully examine the subtle inner workings of models, assessing the merits of different choices for model specification. The pioneers of the field such as Riley, Steele and Fasham played extensively with their (simple) models, trying out different formulations and parameterisations, just to see what would happen. The simplicity afforded by using a zero-dimensional slab physics framework provides an ideal playground for familiarisation with ecosystem models, allowing for a multiplicity of runs and ease of analysis.

Here, we have presented an efficient plankton modelling testbed, EMPOWER, coded in the freely available language R. It provides a readily available and easy to use tool for evaluating model structure, formulations and parameterisations. EMPOWER has several advantages in that it is fast, easy to run, results are straightforward to analyse and, last but by no means least, the code is transparent and easily adapted to incorporate new formulations and parameterisations. As such, the main purpose of EMPOWER is to provide an ecosystem model testbed that allows users to fully familiarise themselves with their models, allowing them to subsequently be incorporated with greater confidence into 1-D or 3-D models, as required. It may be that some amount of reparameterisation is required when transferring the model ecosystem between physical codes, but this ought usually to be minimal in extent and will itself be greatly informed by the previous slab modelling work. Much better this approach, than starting out from scratch using computationally expensive and time-consuming 1-D or 3-D codes to undertake ecosystem model parameterisation.

In order to demonstrate the utility of EMPOWER, we carried out both a parameter tuning exercise and a structural sensitivity analysis, the latter examining the equations for calculating daily depth-integrated photosynthesis, and mortality terms for both phytoplankton and zooplankton. In the parameter tuning exercise, a simple NPZD model, broadly based on the ecosystem model of Fasham (1993), was fitted to data (seasonal cycles) for chlorophyll and nitrate at four stations: India (60° N, 20° W), Biotrans (47° N, 20° W), Papa (50° N, 145° W) and Kerfix (50°40′ S, 68°25′ E). Formal parameter sensitivity analysis was carried out, highlighting which parameters phytoplankton stocks and nitrate drawdown are sensitive to. The model was successfully tuned to all four stations, the two HNLC stations (Papa and Kerfix) requiring different parameterisations, notably a halving of maximum photosynthetic rate (acting as a proxy for iron limitation) relative to the North Atlantic sites.

The parameterisation of the different stations highlighted the somewhat ad hoc process that most modellers go through when assigning parameter values. Some parameters may be set directly from the results of observation and experiment. More often than not, however, the “path of least resistance” when assigning parameters is to simply select values from previously published modelling studies. Equations for processes such as photosynthesis, grazing and mortality can likewise be selected “on-the-shelf” from the published literature. Previous publication does not, of course, guarantee that equations or parameter values are necessarily best suited for a particular modelling application. Moreover, it is all too easy for less than ideal, even dysfunctional, formulations to become entrenched within the discipline and used in common practice (Anderson and Mitra, 2010). As a result, parameter tuning is almost inevitable in ecosystem modelling and we have shown how rigorous sensitivity analysis can help in this regard. Of course, even with a table of parameter sensitivities, there is still a considerable subjective element to choosing which parameters to adjust. The most sensitive parameters should be selected, but the degree of uncertainty in parameter values is an additional consideration. It is no good tuning a sensitive parameter if its value is already well known from observation and experiment.

A necessary complement when ensuring that models show acceptable agreement with data is to remember that it is important that the theories and assumptions underlying the conceptual description of models are correct, or at least not *incorrect* (Rykiel, 1996). Indeed, it is the conceptual realisation of models that in many ways poses the greatest challenge, requiring expertise and practice to overcome observational or experimental lacunae (Tsang, 1991). Subsequent to the parameter tuning exercise, we studied the sensitivity of the Station India simulation to chosen formulations for depth-integrated photosynthesis and both phytoplankton and zooplankton mortality. In the case of the photosynthesis calculation, some aspects showed relatively low sensitivity, namely the choice of *P–I* curve and whether to assume a triangular or sinusoidal pattern of irradiance throughout the day. In contrast, the way in which light attenuation in the water column is calculated showed marked sensitivity. Using a simple Beer's Law attenuation coefficient throughout the water column is clearly oversimplified because the spectral properties of irradiance vary with depth. Moving to a piecewise Beer's Law with separate attenuation coefficients for depth ranges 0–5, 5–23 and > 23 m (Anderson, 1993) led to more rapid light attenuation near the ocean surface. Depth-integrated photosynthesis declined accordingly, delaying the onset of the spring bloom and reducing its magnitude, along with drawdown of nutrient. The difference is of course in part due to parameter values, rather than the inherent difference in the equations. Additional sensitivity analysis and parameter tuning could be used to investigate this further but in fact such an analysis was undertaken by Anderson (1993) who showed that no amount of parameter tuning can adequately account for the fact that attenuation will vary with depth, and cannot be assumed to be constant, because of the spectral properties of the irradiance field. In contrast to the sensitivity seen to equations for light attenuation, choice of *P–I* curve made only a negligible difference to model predictions.

When it comes to biogeochemical modelling studies in GCMs, it is possible that all manner of different methods are used to calculate light attenuation in the water column and resulting photosynthesis. Methodologies are often not reported in full within published texts, the assumption being that they are in some way routine and straightforward and that, perhaps, the models are insensitive to this choice. Consider, for example, the MEDUSA-2.0 model (Yool et al., 2013a), published within *Geoscientific Model Development* and afforded a detailed description of equations and chosen parameter values. Despite this level of detail, the model's calculation of light attenuation is largely overlooked and the reader is instead summarily directed to the LOBSTER model (Levy et al., 2001). This divides light into two wavebands, "red" and "green-blue" that are attenuated separately by seawater, and a Smith function (Eq. 7) is used to calculate photosynthesis. But the published description omits a number of key details (although the model code was supplied), for instance that there is a 50 : 50 division of light between the two wavebands at the ocean surface, that the photosynthetically active fraction is 0.43 of total irradiance, that extinction coefficients for the two wavebands are a function of chlorophyll and that photosynthesis is calculated within each model layer (the model uses fixed layer depths, with 13 layers in the upper 100 m) as a function of average light within the layer.

As a point of interest, we ran our model for station India again, this time using the MEDUSA-2.0 method of light attenuation and a Smith function for the *P*–*I* curve (see Appendix E for details of the parameterisation of light attenuation). The calculation included replication the layer structure within the GCM in order to achieve a full comparison. Results (not shown) were almost identical to the baseline simulation for station India (Fig. 9) for all four state variables, with the minor exception that nitrate drawdown was slightly greater (0.5 mmol N m^{-3}) with the MEDUSA parameterisation. The similarity between the two simulations is because, remarkably, calculated light attenuation using the two red and green wavebands (MEDUSA) differs little from that using the Anderson (1993) piecewise Beer's law. Here, in a nutshell, is a classic example of the utility of EMPOWER. This result should alert GCM modellers to the fact that near identical results can be generated for light attenuation in the water column using these two contrasting sets of equations and a choice can be made as to which is most suitable for implementation based on computational efficiency. From a theoretical point of view, the result is also interesting. The equations of Anderson (1993) are an empirical approximation of the full spectral model of Morel (1988) which divided PAR into 61 wavebands. It would appear that this model can be stripped down to just two wavebands, red and green, without serious degradation in accuracy when it comes to predicting light attenuation.

We also used EMPOWER to undertake an analysis of model sensitivity to the presence/absence of linear and nonlinear mortality terms for phytoplankton and zooplankton. Whereas the use of linear phytoplankton mortality terms is commonplace in models, we investigated the performance of an additional quadratic phytoplankton mortality term. This term is intended to represent loss processes that scale with phytoplankton biomass that are not already accounted for in the model. Given that both self-shading and grazing are explicitly modelled, we considered the quadratic term to represent mortality due to viruses. Model results were sensitive to this parameterisation, highlighting the potential importance of viruses in marine systems, which is consistent with field evidence (Bratbak, 1993, 1996; Danovaro et al., 2011).

It has long been recognized that the parameterisation and functional form of zooplankton mortality, the model closure term, can have a pronounced effect on modeled ecosystem dynamics (e.g. Steele and Henderson, 1981, 1992, 1995; Murray and Parslow, 1999; Edwards and Yool, 2000; Neubert et al., 2004). Quadratic closure is a common choice, although other non-linear functional forms are also in use. While it is commonly stated that quadratic closure is dynamically stabilising, i.e., it prevents both blooms and extinction of prey, there is a limit to this influence (Edwards and Yool, 2000) since other processes can come into play. In our case, it is obvious that quadratic closure had a stabilising effect on the model. Its removal caused the bloom peak to be higher and also post-bloom phytoplankton levels to decline to near-zero.

In contrast to the community's broad recognition of the potential sensitivity to choice of closure scheme, far less attention has been paid to model sensitivity regarding the fate of zooplankton mortality. There are likely various sources of zooplankton in reality including grazing by higher predators, starvation or disease. One can consider the grazing loss to be partitioned between an infinite series of higher predators (e.g., Fasham et al., 1990), with partitioning between detritus and dissolved nutrients in both organic and inorganic form. These fates will occur with time delays and potentially also with spatial separation due to migration of predators. Moreover, any detrital production by higher predators would comprise significantly larger "particles" than those due to plankton death, and would therefore be associated with much higher sinking rates. Non-grazing mortality might lead to production of detritus in situ. There is no consensus on best practice, despite the fact that different approaches to partitioning of zooplankton losses can have a significant effect on modelled ecosystem function. Future structural sensitivity studies should be conducted to explore how the f ratio (the fraction of primary production fuelled by external nutrient) and e ratio (i.e. relative export to total primary production) are affected by the various assumptions relating to zooplankton mortality and model closure.

We have described the utility of slab models as a testbed underpinning marine ecosystem modelling research. This is however by no means their only use. Slab models are ideal for teaching ecological modelling. They embrace the complex interplay between primary production and the physical-chemical environment, combined with top-down control by zooplankton. Students often have difficulty grasping the relative significance of causal effects in ecosystems (Grotzer and Basca, 2003), e.g. the relative roles of bottom-up vs. top-down processes in structuring food webs. A certain amount of lecture material is of course needed, but there is no substitute for hands-on modelling, providing an interactive approach whereby students can actively investigate ideas and interact between themselves and a teacher (Knapp and D'Avanzo, 2010). Insight can be gained by getting students to try simple things like switching grazing off, doubling phytoplankton growth rates, etc. The slab modelling framework provided herein is ideal for this purpose. The code is transparent, modular and readily adjusted to include alternate parameterisations, it is easily set up for alternate ocean sites, the model runs fast with graphs of results appearing on the screen on completion, results are readily written to output files for more in depth analysis and, by coding in R, the models can be accessed and run without need for purchasing proprietary software.

Finally, the great advances in marine ecology that the pioneers of plankton modelling achieved using slab models should not be forgotten. Riley, Steele and Fasham laid the foundations of today's marine ecosystem modelling using plankton models embedded within simple physics. Even in the modern arena, this use of simple physics cannot be dismissed as being too simple for practical application and there is no reason why further scientific advances cannot be made on this basis. Models are, fundamentally, all about simplifying reality.

Appendix A: Irradiance calculations

Both the Evans and Parslow (1985) and Anderson (1993) subroutines for calculating daily photosynthesis require noon irradiance and daylength as inputs. When there are data available, these data can be used as forcing for a model, akin to what is done for temperature. However, most typically light data is not available and so a light submodel must be used to prescribe the light forcing. A climatological approach is often used whereby these inputs are specified using trigonometric/astronomical equations. This task is not as straightforward as it might first appear. The basic equations are presented in texts such as Brock (1981) and Iqbal (1983). Some adjustments were provided by Shine (1984) and we recommend the equation for short-wave irradiance at the ocean surface on a clear day published therein:

$$I_{\text{clear}} = \frac{I_{\text{SC}}\cos^2(z)/R_{\text{V}}^2}{1.2\cos(z) + e_0(1.0 + \cos(z))/1000 + 0.0455} \tag{A1}$$

I_{SC} is the solar constant (e.g., $1368\,\text{W}\,\text{m}^{-2}$: Thekaekara and Drummond, 1971), i.e., the incoming solar radiation that would be incident on a perpendicular plane, immediately outside the atmosphere. I_{clear} also depends on solar zenith angle (z), the Earth's radius vector (R_{V}: accounts for the eccentricity of the earth's orbit) and water vapour pressure (e_0; the partial pressure of water vapour in the atmosphere). A typical value for e_0 is

12 mb (e.g., Josey et al., 2003); the calculation of I_{clear} is not sensitive to this parameter. The equation for R_{V} is:

$$R_{\mathrm{V}} = 1/(1 + 0.033\cos(2\pi J/365))^{1/2} \tag{A2}$$

where J is day of year (Julian day; i.e. 1 = 1 January). Solar zenith angle depends on latitude (φ), solar declination angle (δ) and on time of day (γ, where the Earth moves $15^\circ\,\mathrm{h}^{-1}$ and γ is difference from noon):

$$\cos(z) = \sin(\varphi)\sin(\delta) + \cos(\varphi)\cos(\delta)\cos(\gamma) \tag{A3}$$

The $\cos(\gamma)$ term becomes irrelevant when considering noon irradiance. Solar declination angle is given by:

$$\delta = 23.45\sin(2\pi(284 + J)/365) \tag{A4}$$

where h is hour angle which is the difference between the given time and noon (where 1 h is 15°). Note that δ is expressed in degrees in the above equation (1 radian = $180/\pi$ degrees).

The flux of photosynthetically active solar radiation just below the ocean surface at noon, I_{noon}, can now be calculated:

$$I_{\mathrm{noon}} = C_{\mathrm{FAC}} f_{\mathrm{PAR}} (1 - \phi) I_{\mathrm{clear}} \tag{A5}$$

where f_{PAR} is the fraction of solar radiation that is PAR (λ between 400 and 700 nm), ϕ is ocean albedo and C_{FAC} is the effect of clouds on atmospheric transmission. Parameters f_{PAR} and ϕ are relatively invariant with typical values of 0.43 for f_{PAR} and 0.04 for ϕ (e.g., Fasham et al., 1990). Dealing with the effects of clouds is a thorny issue for modellers.

Simple empirical approaches have been developed, two of the most popular being those of Reed (1977) and Smith and Dobson (1984). We have opted for the former in which C_{FAC} is a function of zenith angles (specified in degrees):

$$C_{\mathrm{FAC}} = 1 - 0.62W/8 + 0.0019(90 - z) \tag{A6}$$

5 where W is cloud fraction in oktas. A value of $W = 6$ was used for all four stations.

Appendix B: Analytic integrals for photosynthesis with depth

The average photosynthesis within a layer of depth H is:

$$\overline{V}_{P(H)} = \frac{1}{H}\int_{z=0}^{H} V_P(z)\mathrm{d}z \tag{B1}$$

where V_P is photosynthesis as a function of light intensity (specified as the P–I curve). 10 Two P–I curves are provided with EMPOWER, a Smith function (Eq. 7) and exponential function (Eq. 8). Analytic solutions to Eq. (B1) are provided here for each of these two P–I curves. In both cases a Beer's law attenuation with depth is assumed (parameter k_{PAR}), i.e., $I(z) = I(0)e^{-k_{\mathrm{PAR}}z}$ where $I(0)$ is the irradiance entering the layer from above.

B1 Smith P–I curve

15 By performing a change of variables such that $x = \alpha I(z)$, the integral above becomes:

$$\overline{V}_{P(H)} = \frac{-V_P^{\max}}{H}\int_{z=0}^{H} \frac{1}{\left(\left(V_P^{\max}\right)^2 + x^2\right)^{1/2}}\mathrm{d}x \tag{B2}$$

This integral is solved analytically using a trigonometric transformation and then integration by parts, giving:

$$\overline{V}_{P(H)} = \frac{V_P^{\max}}{k_{\mathrm{PAR}} H} \ln \left(\frac{x_0 + \left((V_P^{\max})^2 + x_0^2 \right)^{1/2}}{x_H + \left((V_P^{\max})^2 + x_H^2 \right)^{1/2}} \right) \tag{B3}$$

where x_0 is $x(z=0)$ and x_H is $x(z=H)$.

B2 Exponential *P–I* curve

In order to integrate Eq. (B1) using an exponential *P–I* curve it is first useful to define (Platt et al., 1980):

$$I_*^z = \frac{I_z \alpha}{V_P^{\max}} \tag{B4}$$

The integration over depth is then (see Platt et al., 1990):

$$\overline{V}_{P(H)} = \frac{V_P^{\max}}{k_{\mathrm{PAR}} H} \sum_{n=1}^{\infty} \frac{(-1)^{n+1}}{n \cdot n!} \left(\left(I_*^0 \right)^n - (I_*^H)^n \right) \tag{B5}$$

For practical purposes, we used a maximum value of n of 16.

Appendix C: Special formulations for calculating daily photosynthesis

C1 Evans and Parslow (1985) photosynthesis calculation

Evans and Parslow (1985) provide an algorithm for calculating daily depth-integrated photosynthesis with the assumptions of a Smith *P–I* curve (Eq. 3), a triangular pattern of irradiance from sunrise to sunset and light extinction calculated with a single Beer's law coefficient. The average daily rate of photosynthesis within the mixed layer is calculated as:

$$\overline{V}_{P(H,\tau)} = 2\int_0^\tau \frac{1}{H}\int_0^M V_P(I,z)\,\mathrm{d}z\,\mathrm{d}t \tag{C1}$$

where t, measured in days, is 0 at sunrise and τ at noon and H is layer depth. Assuming a triangular pattern of irradiance about noon, Eq. (C1) can be recast as (Evans and Parslow, 1985):

$$\overline{V}_{P(H,\tau)} = \frac{2V_P^{\max}}{k_{\mathrm{PAR}}H}\int_0^\tau\int_{\beta 1}^{\beta 2} \frac{t\cdot \mathrm{d}y\cdot \mathrm{d}t}{y(y^2+t^2)^{1/2}} \tag{C2}$$

$$\beta_1 = \frac{V_P^{\max}\tau}{\alpha I_{\mathrm{noon}}}, \beta_2 = \beta_1\exp(k_{\mathrm{PAR}}H) \tag{C3}$$

I_{noon} is the photosynthetically active radiation (PAR) just below the ocean surface at noon. This integral solves as (Evans and Parslow, 1985):

$$\overline{V}_{P(H,\tau)} = \frac{2V_P^{\max}}{k_{\mathrm{PAR}}H}\left[f(\beta_{2,}\tau) - f(\beta_{1,}\tau) - f(\beta_{2,}0) + f(\beta_1,0)\right] \tag{C4}$$

$$f(y,t) = (y^2+t^2)^{1/2} - t \cdot \ln\frac{t+(y^2+t^2)^{1/2}}{y} \tag{C5}$$

C2 Anderson (1993) photosynthesis calculation

The subroutine of Anderson (1993) was developed as an empirical approximation to the spectrally resolved model of light attenuation and photosynthesis of Morel (1988) used in combination with the polynomial method of integrating daily photosynthesis of Platt et al. (1990). It is based on an exponential *P*–*I* curve (Eq. 8), assumes a sinusoidal pattern of irradiance throughout the day and calculated light attenuation using a piecewise Beer's law (Eq. 10). The irradiance leaving the base of each layer is:

$$I_{\mathrm{base},i} = I_{\mathrm{base},i-1}\exp[-k_{\mathrm{PAR},i}(z_{\mathrm{base},i} - z_{\mathrm{base},i-1})] \tag{C6}$$

where $I_{\mathrm{base},0}$ is the irradiance immediately below the ocean surface and $z_{\mathrm{base},i}$ is the depth of the base of the layer i (where $z_{\mathrm{base},0} = 0$).

The subroutine of Anderson (1993) also takes account of the fact that, in reality, α depends on the spectral properties of light and therefore varies with depth in the water column. This parameter is the product of photosynthetic absorption cross section $a_{\mathrm{c}}(\lambda)$, which is spectrally dependent (λ denotes wavelength), and quantum yield φ_{A} (Platt and Jassby, 1976; Platt, 1986):

$$\alpha(\lambda) = a_c(\lambda)\varphi_A \tag{C7}$$

Ordinarily (e.g., Table 2), α is the initial slope of the P–I curve for white light (i.e., spectral distribution as for irradiance at the ocean surface). The corresponding value of α for the wavelength at which absorption is maximum, α_{max}, is (Anderson, 1993):

$$\alpha_{\text{max}} = 2.602\alpha \tag{C8}$$

The value of α for any given wavelength of PAR, $\alpha(\lambda)$, is then:

$$\alpha(\lambda) = \alpha_{\text{max}} a^*(\lambda) \tag{C9}$$

where $a^*(\lambda)$ is the dimensionless chlorophyll absorption cross section for wavelength λ. An additional complication, however, is that $a^*(\lambda)$ only applies when irradiance is specified as a scalar flux (Morel, 1991). Irradiance in the model is a downwelling flux and so Anderson (1993) converted between the two by defining a new version of the chlrophyll absorption cross section (which can be used in Eq. (C9) in place of $a^*(\lambda)$, in combination with downwelling irradiance):

$$\alpha^{\#}(\lambda) = a^*(\lambda) k_{\text{PAR}}(\lambda)/a_c(\lambda) \tag{C10}$$

Again using the piecewise three-layer scheme described above for k_{PAR}, an average value of $a^{\#}$ can be calculated for each layer by deriving an empirical approximation of Morel's (1988) full spectral model. As a first step, $a^{\#}$ at the ocean surface is calculated as:

$$a^{\#}_{\text{base},0} = h_0 + h_1 C^{1/2} + h_2 C + h_3 C^{3/2} + h_4 C^2 \tag{C11}$$

where the polynomial coefficients are given in Table C1. The $a^{\#}$ at the base of each layer and the average $a^{\#}$ in each layer are then calculated as:

$$a^{\#}_{\mathrm{base},i} = \alpha^{\#}_{\mathrm{base},i-1} + \alpha^{\#}_{\mathrm{calc},i} \tag{C12}$$

$$a^{\#}_{\mathrm{av},i} = \alpha^{\#}_{\mathrm{base},i-1} + 0.5\alpha^{\#}_{\mathrm{calc},i} \tag{C13}$$

where $a^{\#}_{\mathrm{calc},i}$ is a lengthy empirical calculation:

$$a^{\#}_{\mathrm{calc},i} = f\{z_{\mathrm{base},i}\} - f\{z_{\mathrm{base},i-1}\} \tag{C14}$$

$$\begin{aligned} f\{z\} = {} & (z+1)\left(g_1 + g_2 C^{1/2} + g_5 C + g_7 C^{3/2}\right) + f_1\{z+1\}(g_3 + g_4 C^{1/2} + g_9 C) \\ & + f_2\{z+1\}(g_6 + g_{10} C) + f_3\{z+1\} g_8 \end{aligned} \tag{C15}$$

$$f_1\{z+1\} = (z+1)\ln(z+1) - (z+1) \tag{C16}$$

$$f_2\{z+1\} = (z+1)\ln^2(z+1) - 2f_1\{z+1\} \tag{C17}$$

$$f_3\{z+1\} = (z+1)\ln^3(z+1) - 3f_2\{z+1\} \tag{C18}$$

The coefficients, g_x, are provided in Table C1. With irradiance assumed to vary sinusoidally through the day, the average rate of photosynthesis within a layer i is:

$$\overline{V}_{P(H,\tau)} = \frac{DV_P^{\max}}{24H\pi k_{\mathrm{PAR}}} \sum_{j=1}^{5} \Omega_j (V_1^j - V_2^j) \tag{C19}$$

$$V_1 = \alpha_{\max} a^{\#}_{\mathrm{av},i} I_{\mathrm{base},i-1} / V_P^{\max} \tag{C20}$$

$$V_2 = \alpha_{\max} a^{\#}_{\mathrm{av},i} I_{\mathrm{base},i} / V_P^{\max} \tag{C21}$$

where D is daylength (hours) and Ω_j are the polynomial coefficients (Platt et al., 1990; Table C1).

Appendix D: EMPOWER1.0 User guide

1. *Installation and setup*. The R programming language is freeware and is readily downloaded from the web for use on personal computers. For example, visit page: http://www.r-project.org/. After installation, set up a directory to hold the model code and associated input and output files. We recommend also downloading an R editor, e.g, Tinn-R (also freeware).

2. *Running R*. Open the R console. From the toolbar, select “File” and “Change dir . . . ” and select the directory in which the model code and input files have been placed. To run the model, type: source(“EMPOWER1.R”)

3. *Preparation of input files*. The model reads in three input files, each as ASC II text files:

    i. File NPZD_parms.txt. This file includes a single line header and then lists the value of each model parameter in turn, followed by a text string for the purpose of annotation. When changing the parameter list in the model, the corresponding section in the R code must be altered accordingly.

    ii. File NPZD_extra.txt. This file holds initial values for state variables, additional parameters, and various flags: choice of station, choices for photosynthesis calculations (*P*–*I* curve, light attenuation, etc.) and grazing formulation. The user is at liberty to add to or remove from this list of flags as is desired. This file also contains flags for core model functions: run duration, time step, output type (none, last year, whole simulation), output frequency and integration method (Euler or Runge Kutta). These latter functions are required by the core code and should not be removed from this file.

    iii. File stations_forcing.txt. This file has a header line for information, and then holds monthly values for forcing, in our case mixed layer depth and temperature, for each station. There are thirteen entries in each case, the first and last being the same and corresponding to the beginning and end of the year. A 366 unit array is set up in the model code for each forcing variable, with unit 1 corresponding to $t = 0$, and linear interpolation carried out on the monthly values to fill each array.

4. *Output files*. These are generated automatically by the model, on completion of each model simulation. The type of output generated is controlled by flags (above). The output files are ASC II, comma separated and do not have headers. They are readily imported into various software packages, e.g. R or Microsoft Excel, for further analysis. The files are:

   i. File out_statevars.txt. Outputs the state variables, ordered as they are in array X in the code.

   ii. File out_fluxes.txt. Outputs the model fluxes, ordered as they are in matrix flux (i, j) in function FNget_flux. Thus each line (corresponding to a point in time for output) has Nsvar*nfluxmax entries where Nsvar is the number of state variables in the model and nfluxmax is the maximum number of fluxes per state variable.

   iii. File out_aux.txt. This file stores the values of auxiliary variables, as defined by the user in array Y (final section of function FNget_flux). The maximum size of this array is set by variable nDvar.

5. *Altering the model structure*. If the user wants to change the number of state variables, or nDvar or nfluxmax (above), adjustments should first be made to the short section of code “Variables specific to model: adjust accordingly”. Alter nSvar, the initialisation of array X (which holds the state variables) and the text arrays svarname and svarnames (which are used for output). Then go to function FNget_flux and rewrite the line of code unpacking the state variables. Finally, specify the terms associated with the new state variable(s) in matrix flux (i, j).

6. *Altering model equations*. The model equations are handled in function FNget_flux and can be adjusted as desired by the user, calling additional functions as necessary.

7. *Graphical output*. The model automatically generates graphical output on the computer screen on completion of each simulation. An advantage of R is that the syntax for generating plots is straightforward and the user should have no problem, working from the plots provided, in generating extra graphs, as desired.

Appendix E: Light attenuation in MEDUSA

Light attenuation in the water column in the MEDUSA model (Yool et al., 2011, 2013) is calculated assuming that PAR at the ocean surface can be divided equally into two wavebands, nominally red and green. The attenuation of each is calculated through the water column using Beer's law. The average light in a model layer can then be calculated on the basis of summing the two wavebands, and this average then used in combination with a *P–I* curve to calculate photosynthesis. The extinction coefficients for red and green light, xkr and xkg, are:

$$\mathrm{xkr} = \mathrm{xkr0} + \mathrm{xkrp}.\exp(\mathrm{xlr}.\ln(C)) \tag{E1}$$

$$\mathrm{xkg} = \mathrm{xkg0} + \mathrm{xkgp}.\exp(\mathrm{xlg}.\ln(C)) \tag{E2}$$

where C is chlorophyll (mg m^{-3}). Values for the coefficients are: xkr0 = 0.225, xkrp = 0.037, xlr = 0.674, xkg0 = 0.0232, xkgp = 0.074, xlg = 0.629.

The Supplement related to this article is available online at doi:10.5194/gmdd-8-53-2015-supplement.

Acknowledgements. T. R. Anderson and A. Yool acknowledge support from the Natural Environment Research Council, UK, as part of the Integrated Marine Biogeochemical Modelling

Network to Support UK Earth System Research (i-MarNet) project (grant ref. NE/K001345/1). W. C. Gentlemen acknowledges support from the Natural Sciences and Engineering Council of Canada.

References

Anderson, T. R.: A spectrally averaged model of light penetration and photosynthesis, Limnol. Oceanogr., 38, 1403–1419, 1993.

Anderson, T. R.: Relating C : N ratios in zooplankton food and faecal pellets using a biochemical model, J. Exp. Mar. Biol. Ecol., 184, 183–199, 1994.

Anderson, T. R.: Plankton functional type modelling: running before we can walk?, J. Plankton Res., 27, 1073–1081, 2005.

Anderson, T. R.: Progress in marine ecosystem modelling and the "unreasonable effectiveness of mathematics", J. Marine Syst., 81, 4–11, 2010.

Anderson, T. R. and Gentleman, W. C.: The legacy of Gordon Arthur Riley (1911–1985) and the development of mathematical models in biological oceanography, J. Mar. Res., 70, 1–30, 2012.

Anderson, T. R. and Hessen, D. O.: Carbon or nitrogen limitation in marine copepods?, J. Plankton Res., 17, 317–331, 1995.

Anderson, T. R. and Mitra, A.: Dysfunctionality in ecosystem models: an underrated pitfall?, Prog. Oceanogr., 84, 66–68, 2010.

Anderson, T. R. and Pondaven, P.: Non-Redfield carbon and nitrogen cycling in the Sargasso Sea: pelagic imbalances and export flux, Deep-Sea Res. Pt. I, 50, 573–591, 2003.

Anderson, T. R., Gentleman, W. C., and Sinha, B.: Influence of grazing formulations on the emergent properties of a complex ecosystem model in a global general circulation model, Prog. Oceanogr., 87, 201–213, 2010.

Anderson, T. R., Hessen, D. O., Mitra, A., Mayor, D. J., and Yool, A.: Sensitivity of secondary production and export flux to choice of trophic transfer formulation in marine ecosystem models, J. Marine Syst., 125, 41–53, 2013.

Anderson, T. R., Christian, J. R., and Flynn, K. J.: Modeling DOM biogeochemistry, in: Biogeochemistry of Marine Dissolved Organic Matter, 2nd Edn., edited by: Hansell, D. A. and Carlson, C. A., Academic Press, 635–667, 2014.

Antonov, J. I., Seidov, D., Boyer, T. P., Locarnini, R. A., Mishonov, A. V., Garcia, H. E., Baranova, O. K., Zweng, M. M., and Johnson, D. R.: World Ocean Atlas 2009, Volume 2: Salinity, edited by: Levitus, S., NOAA Atlas NESDIS 69, US Government Printing Office, Washington, DC, 184 pp., 2010.

Arhonditsis, G. B., Adams-Vanharn, B. A., Nielsen, L., Stow, C. A., and Reckhow, K. H.: Evaluation of the current state of mechanistic aquatic biogeochemical modeling: citation analysis and future perspectives, Environ. Sci. Technol., 40, 6547–6554, 2006.

Backhaus, J. O., Hegseth, E. N., Wehde, H., Irigoien, X., Hatten, K., and Logemann, K.: Convection and primary production in winter, Mar. Ecol.-Prog. Ser., 251, 1–14, 2003.

Blackford, J. C., Allen, J. I., and Gilbert, F. J.: Ecosystem dynamics at six contrasting sites: a generic modelling study, J. Marine Syst., 52, 191–215, 2004.

Boushaba, K. and Pascual, M.: Dynamics of the “echo” effect in a phytoplankton system with nitrogen fixers, B. Math. Biol., 67, 487–507, 2005.

Bratbak, G., Egge, J. K., and Heldal, M.: Viral mortality of the marine alga *Emiliania huxleyi* (Haptophyceae) and termination of algal blooms, Mar. Ecol.-Prog. Ser., 93, 39–48, 1993.

Bratbak, G., Willson, W., and Heldal, M.: Viral control of *Emiliania huxleyi* blooms?, J. Marine Syst., 9, 75–81, 1996.

Brock, T. D.: Calculating solar radiation for ecological studies, Ecol. Model., 14, 1–19, 1981.

Chai, F., Lindley, S. T., Toggweiler, J. R., and Barber, R. T.: Testing the importance of iron and grazing in the maintenance of the high nitrate condition in the equatorial Pacific Ocean, a physical-biological model study, in: The Changing Ocean Carbon Cycle, edited by: Hanson, R. B., Ducklow, H. W., Field, J. G., International Geosphere–Biosphere Programme (IGBP) Book Series 5, Cambridge University Press, Cambridge, 156–186, 2000.

Coale, K. H., Johnson, K. S., Fitzwater, S. E., Gordon, R. M., Tanner, S., Chavez, F. P., Ferioli, L., Sakamoto, C., Rogers, P., Millero, F., Steinberg, P., Nightingale, P., Cooper, D., Cochlan, W. P., Landry, M. R., Constantinou, J., Rollwagen, G., Trasvina, A., and Kudela, R.: A massive phytoplankton bloom induced by an ecosystem-scale iron fertilization experiment in the equatorial Pacific Ocean, Nature, 838, 495–501, 1996.

Cullen, J. J.: On models of growth and photosynthesis in phytoplankton, Deep-Sea Res., 37, 667–683, 1990.

Danovaro, R., Corinaldesi, C., Dell’Anno, A., Fuhrman, J. A., Middelburg, J. J., Noble, R. T., and Suttle, C. A.: Marine viruses and global climate change, FEMS Microbiol. Rev., 35, 933–1034, 2011.

Edwards, A. M. and Yool, A.: The role of higher predation in plankton population models, J. Plankton Res., 22, 1085–1112, 2000.

Eppley, R. W.: Temperature and phytoplankton growth in the sea, Fish. Bull. Nat. Ocean Atmos. Adm., 70, 1063–1085, 1972.

Eppley, R. W. and Peterson, B. J.: Particulate organic matter flux and planktonic new production in the deep ocean, Nature, 282, 677–680, 1979.

Evans, G. T. and Parslow, J. S.: A model of annual plankton cycles, Biol. Oceanogr., 3, 327–347, 1985.

Fasham, M. J. R.: Modelling the marine biota, in: The Global Carbon Cycle, edited by: Heimann, M., NATO ASI Series Vol. I15, 457–504, 1993.

Fasham, M. J. R.: Variations in the seasonal cycle of biological production in subarctic oceans: a model sensitivity analysis, Deep-Sea Res. Pt. I, 42, 1111–1149, 1995.

Fasham, M. J. R., Ducklow, H. W., and McKelvie, S. M.: A nitrogen-based model of plankton dynamics in the oceanic mixed layer, J. Mar. Res., 48, 591–639, 1990.

Fennel, K., Losch, M., Schröter, J., and Wenzel, M.: Testing a marine ecosystem model: sensitivity analysis and parameter optimization, J. Marine Syst., 28, 45–63, 2001.

Findlay, H. S., Yool, A., Nodale, M., and Pitchford, J. W.: Modelling of autumn plankton bloom dynamics, J. Plankton Res., 28, 209–220, 2006.

Fleming, R. H.: The control of diatom populations by grazing, J. Cons. Int. Expl. Mer., 14, 210–227, 1939.

Follows, M. J., Dutkiewicz, S., Grant, S., and Chisholm, S. W.: Emergent biogeography of microbial communities in a model ocean, Science, 315, 1843–1846, 2007.

Friedrichs, M. A. M., Dusenberry, J. A., Anderson, L. A., Armstrong, R. A., Chai, F., Christian, J. R., Doney, S. C., Dunne, J., Fujii, M., Hood, R., McGillicuddy, D. J., Moore, K. J., Schartau, M., Spitz, Y. H., and Wiggert, J. D.: Assessment of skill and portability in regional marine biogeochemical models: role of multiple planktonic groups, J. Geophys. Res., 112, C08001, doi:10.1029/2006JC003852, 2007.

Frost, B. W.: Grazing control of phytoplankton stock in the open subarctic Pacific Ocean: a model assessing the role of mesozooplankton, particularly the large calanoid copepods *Neocalanus* spp, Mar. Ecol.-Prog. Ser., 39, 49–68, 1987.

Fussmann, G. F. and Blasius, B.: Community response to enrichment is highly sensitive to model structure, Biol. Letters, 1, 9–12, 2005.

Garcia, H. E., Locarnini, R. A., Boyer, T. P., Antonov, J. I., Zweng, M. M., Baranova, O. K., and Johnson, D. R.: World ocean atlas 2009, volume 4: nutrients (phosphate, nitrate, silicate), in: NOAA Atlas NESDIS 71, edited by: Levitus, S., US Government Printing Office, Washington, DC, 398 pp., 2010.

Gentleman, W.: A chronology of plankton dynamics *in silico*: how computer models have been used to study marine ecosystems, Hydrobiologia, 480, 69–85, 2002.

Gentleman, W., Leising, A., Frost, B., Strom, S., and Murray, J.: Functional responses for zooplankton feeding on multiple resources: a review of assumptions and biological dynamics, Deep-Sea Res. Pt. II, 50, 2847–2875, 2003.

Gran, H. H.: Phytoplankton. Methods and problems, J. Conseil Int. Expl. Mer., 7, 343–358, 1932.

Gran, H. H. and Braarud, T.: A quantitative study of the phytoplankton in the Bay of Fundy and the Gulf of Maine (including observations on hydrography, chemistry and turbidity), J. Biological Bd. Canada, 1, 279–433, 1935.

Grotzer, T. A. and Basca, B. B.: How does grasping the underlying causal structures of ecosystems impact students' understanding?, J. Biol. Educ., 38, 16–29, 2003.

Harrison, W. G. and Platt, T.: Photosynthesis–irradiance relationships in polar and temperate phytoplankton populations, Polar Biol., 5, 153–164, 1986.

Hashioka, T., Vogt, M., Yamanaka, Y., Le Quéré, C., Buitenhuis, E. T., Aita, M. N., Alvain, S., Bopp, L., Hirata, T., Lima, I., Sailley, S., and Doney, S. C.: Phytoplankton competition during the spring bloom in four plankton functional type models, Biogeosciences, 10, 6833–6850, doi:10.5194/bg-10-6833-2013, 2013.

Hemmings, J. C. P., Srokosz, M. A., Challenor, P., and Fasham, M. J. R.: Split-domain calibration of an ecosystem model using satellite ocean colour data, J. Marine Syst., 50, 141–179, 2004.

Hinckley, S., Coyle, K. O., Gibson, G., Hermann, A. J., and Dobbins, E. L.: A biophysical NPZ model with iron for the Gulf of Alaska: reproducing the differences between an oceanic HNLC ecosystem and a classical northern temperate shelf ecosystem, Deep-Sea Res. Pt. II, 56, 2520–2536, 2009.

Huisman, J., Arrayas, M., Ebert, U., and Sommeijer, B.: How do sinking phytoplankton species manage to persist?, Am. Nat., 159, 245–254, 2002.

Hurtt, G. C. and Armstrong, R. A.: A pelagic ecosystem model calibrated with BATS data, Deep-Sea Res., 43, 653–683, 1996.

Iqbal, M.: An Introduction to Solar Radiation, Academic Press, Toronto, 390 pp., 1983.

Josey, S. A., Pascal, R. W., Taylor, P. K., and Yelland, M. J.: A new formula for determining the atmospheric longwave flux at the ocean surface at mid-high latitudes, J. Geophys. Res., 108, 3108, doi:10.1029/2002JC001418, 2003.

Kawamiya, M., Kishi, M., Yamanaka, Y., and Suginohara, N.: An ecological-physical coupled model applied to Station Papa, J. Oceanogr., 51, 635–664, 1995.

Kearney, K. A., Stock, C., Aydin, K., and Sarmiento, J. L.: Coupling planktonic ecosystem and fisheries food web models for a pelagic ecosystem: description and validation for the subarctic Pacific, Ecol. Model., 237–238, 43–62, 2012.

Kidston, M., Matear, R., and Baird, M. E.: Phytoplankton growth in the Australian sector of the Southern Ocean, examined by optimising ecosystem model parameters, J. Marine Syst., 128, 123–137, 2013.

Kimball, H. H.: Amount of solar radiation that reaches the surface of the earth on the land and on the sea, and methods by which it is measured, Mon. Weather Rev., 56, 393–398, 1928.

Knapp, A. K. and D'Avanzo, C.: Teaching with principles: toward more effective pedagogy in ecology, Ecosphere, 1, 15, 2010.

Landry, M. R., Barber, R. T., Bidigare, R. R., Chai, F., Coale, K. H., Dam, H. G., Lewis, M. R., Lindley, S. T., McCarthy, J. J., Roman, M. R., Stoecker, D. K., Verity, P. G., and White, J. R.: Iron and grazing constraints on primary production in the central equatorial Pacific: an EqPac synthesis, Limnol. Oceanogr., 42, 405–418, 1997.

Landry, M. R., Selph, K. E., Taylor, A. G., Décima, M., Balch, W. M., and Bidigare, R. R.: Phytoplankton growth, grazing and production balances in the HNLC equatorial Pacific, Deep-Sea Res. Pt. II, 58, 524–535, 2011.

Le Quéré, C., Harrison, S. P., Prentice, I. C., Buitenhuis, E. T., Aumont, O., Bopp, L., Claustre, H., Cotrim Da Cunha, L., Geider, R., Giraud, X., Klaas, C., Kohfeld, K. E., Legendre, L., Manizza, M., Platt, T., Rivkin, R. B., Sathyendranath, S., Uitz, J., Watson, A. J., and Wolf-Gladrow, D.: Ecosystem dynamics based on plankton functional types for global ocean biogeochemistry models, Glob. Change Biol., 11, 2016–2040, 2005.

Levy, M., Klein, P., and Treguier, A.-M.: Impacts of sub-mesoscale physics on phytoplankton production and subduction, J. Mar. Res., 59, 535–565, 2001.

Llebot, C., Spitz, Y. H., Solé, J., and Estrada, M.: The role of inorganic nutrients and dissolved organic phosphorus in the phytoplankton dynamics of a Mediterranean bay. A modeling study, J. Marine Syst., 83, 192–208, 2010.

Locarnini, R. A., Mishonov, A. V., Antonov, J. I., Boyer, T. P., Garcia, H. E., Baranova, O. K., Zweng, M. M., and Johnson, D. R.: World Ocean Atlas 2009, Volume 1: Temperature, edited by: Levitus, S., NOAA Atlas NESDIS 68, US Government Printing Office, Washington, DC, 184 pp., 2010.

Martin, J. H. and IronEx team: testing the iron hypothesis in ecosystems of the equatorial Pacific Ocean, Nature, 371, 123–129, 1994.

Matear, R. J.: Parameter optimization and analysis of ecosystem models using simulated annealing: a case study at Station P, J. Mar. Res., 53, 571–607, 1995.

Mitra, A.: Are closure terms appropriate or necessary descriptors of zooplankton loss in nutrient–phytoplankton–zooplankton type models?, Ecol. Model., 220, 611–620, 2009.

Mitra, A., Flynn, K. J., and Fasham, M. J. R.: Accounting for grazing dynamics in nitrogen-phytoplankton-zooplankton models, Limnol. Oceanogr., 52, 649–661, 2007.

Mitra, A., Castellani, C., Gentleman, W. C., Jónasdóttir, S. H., Flynn, K. J., Bode, A., Halsband, C., Kuhn, P., Licandro, P., Agersted, M. D., Calbet, A., Lindeque, P. K., Koppelmann, R., Møller, E. F., Gislason, A., Nielsen, T. G., and St John, M.: Bridging the gap between marine biogeochemical and fisheries sciences; configuring the zooplankton link, Prog. Oceanogr., 129, 176–199, 2014.

Mongin, M., Nelson, D. M., Pondaven, P., and Tréguer, P.: Simulation of upper-ocean biogeochemistry with a flexible-composition phytoplankton model: C, N and Si cycling and Fe limitation in the Southern Ocean, Deep-Sea Res. Pt. II, 53, 601–619, 2006.

Moore, K. J., Doney, S. C., and Lindsay, K.: Upper ocean ecosystem dynamics and iron cycling in a global three-dimensional model, Global Biogeochem. Cy., 18, GB4028, doi:10.1029/2004GB002220, 2004.

Morel, A.: Optical modelling of the upper ocean in relation to its biogenous matter content (case 1 waters), J. Geophys. Res., 93, 10749–10768, 1988.

Morel, A.: Light and marine photosynthesis: a spectral model with geochemical and climatological implications, Prog. Oceanogr., 26, 263–306, 1991.

Murray, A. G. and Parslow, J. S.: The analysis of alternative formulations in a simple model of a coastal ecosystem, Ecol. Model., 119, 149–166, 1999.

Natvik, L.-J., Eknes, M., and Evensen, G.: A weak constraint inverse for a zero-dimensional marine ecosystem model, J. Marine Syst., 28, 19–44, 2001.

Neubert, M. G., Klanjscek, T., and Caswell, H.: Reactivity and transient dynamics of predator-prey and food web models, Ecol. Model., 179, 29–38, 2004.

O'Reilly, J. E., Maritorena, S., Mitchell, B. G., Siegal, D. A., Carder, K. L., Garver, S. A., Kahru, M., and McClain, C.: Ocean color chlorophyll algorithms for SeaWiFS, J. Geophys. Res., 103, 24937–24953, 1998.

Onitsuka, G. and Yanagi, T.: Differences in ecosystem dynamics between the northern and southern parts of the Japan Sea: analyses with two ecosystem models, J. Oceanogr., 61, 415–433, 2005.

Oschlies, A. and Garçon, V.: An eddy-permitting coupled physical-biological model of the North Atlantic 1. Sensitivity to advection numerics and mixed layer physics, Global Biogeochem. Cy., 13, 135–160, 1999.

Oschlies, A. and Schartau, M.: Basin-scale performance of a locally optimized marine ecosystem model, J. Mar. Res., 63, 335–358, 2005.

Platt, T.: Primary production of the ocean water column as a function of surface light intensity algorithms for remote sensing, Deep-Sea Res., 33, 149–163, 1986.

Platt, T. and Jassby, A. D.: The relationship between photosynthesis and light for natural assemblages of coastal marine phytoplankton, J. Phycol., 12, 421–430, 1976.

Platt, T., Gallegos, C. L., and Harrison, W. G.: Photoinhibition of photosynthesis in natural assemblages in marine phytoplankton, J. Mar. Res., 38, 687–701, 1980.

Platt, T., Sathyendranath, S., and Ravindran, P.: Primary production by phytoplankton: analytic solutions for daily rates per unit area of water surface, P. Roy. Soc. Lond. B Bio., 241, 101–111, 1990.

Popova, E. E., Fasham, M. J. R., Osipov, A. V., and Ryabchenko, V. A.: Chaotic behaviour of an ocean ecosystem model under seasonal external forcing, J. Plankton Res., 19, 1495–1515, 1997.

Price, N. M., Ahner, B. A., and Morel, F. M. M.: The equatorial Pacific: grazer controlled phytoplankton populations in an iron-limited ecosystem, Limnol. Oceanogr., 39, 520–534, 1994.

Record, N. R., Pershing, A. J., Runge, J. A., Mayo, C. A., Monger, B. C., and Chen, C.: Improving ecological forecasts of copepod community dynamics using genetic algorithms, J. Marine Syst., 82, 96–110, 2010.

Reed, R. K.: On estimating insolation over the ocean, J. Phys. Oceanogr., 7, 482–485, 1977.

Rey, F.: Photosynthesis–irradiance relationships in natural phytoplankton populations of the Barents Sea, Polar Res., 10, 105–116, 1991.

Riley, G. A.: Factors controlling phytoplankton populations on Georges Bank, J. Mar. Res., 6, 54–73, 1946.

Riley, G. A., Stommel, H., and Bumpus, D. F.: Quantitative ecology of the plankton of the western North Atlantic, Bull. Bingham Oceanogr. Coll., 12, 1–169, 1949.

Riley, J. S., Sanders, R., Marsay, C., Le Moigne, F. A. C., Achterberg, E. P., and Poulton, A. J.: The relative contribution of fast and slow sinking particles to ocean carbon export, Global Biogeochem. Cy., 26, GB1026, doi:10.1029/2011GB004085, 2012.

Robinson, C. L. K., Ware, D. M., and Parsons, T. R.: Simulated annual plankton production in the northeastern Pacific coastal upwelling domain, J. Plankton Res., 15, 161–183, 1993.

Rykiel Jr., E. J. : Testing ecological models: the meaning of validation, Ecol. Model., 90, 229–244, 1996.

Salihoglu, B., Garçon, V., Oschlies, A., and Lomas, M. W.: Influence of nutrient utilization and remineralization stoichiometry on phytoplankton species and carbon export: a modeling study at BATS, Deep-Sea Res. Pt. I, 55, 73–107, 2008.

Sathyendranath, S., Stuart, V., Nair, A., Oka, K., Nakane, T., Bouman, H., Forget, M.-H., Maass, H., and Platt, T.: Carbon-to-chlorophyll ratio and growth rate of phytoplankton in the sea, Mar. Ecol.-Prog. Ser., 383, 73–84, 2009.

Schartau, M., Oschlies, A., and Willebrand, J.: Parameter estimates of a zero-dimensional ecosystem model applying the adjoint method, Deep-Sea Res. Pt. II, 48, 1769–1800, 2001.

Shine, K. P.: Parametrization of the shortwave flux over high albedo surfaces as a function of cloud thickness and surface albedo, Q. J. Roy. Meteor. Soc., 110, 747–764, 1984.

Slezak, D. F., Suárez, C., Cecchi, G. A., Marshall, G., and Stolovitzky, G.: When the optimal is not the best: parameter estimation in complex biological models, Plos ONE, 5, 1–10, 2010.

Smith, S. D. and Dobson, F. E.: The heat budget at Ocean Weather Ship Bravo, Atmos. Ocean, 22, 1–22, 1984.

Smith Jr., W. O. and Lancelot, C.: Bottom-up versus top-down control in phytoplankton of the Southern Ocean, Antarct. Sci., 16, 531–539, 2004.

Soetaert, K., Petzoldt, T., and Woodrow, S.: Solving differential equations in R, The R Journal, 2, 5–15, 2010.

Spitz, Y. H., Moisan, J. R., Abbott, M. R., and Richman, J. G.: Data assimilation and a pelagic ecosystem model: parameterization using time series observations, J. Marine Syst., 16, 51–68, 1998.

Spitz, Y. H., Moisan, J. R., and Abbott, M. R.: Configuring an ecosystem model using data from the Bermuda Atlantic Time Series (BATS), Deep-Sea Res. Pt. II, 48, 1733–1768, 2001.

Steele, J. H.: Plant production on the Fladen Ground, J. Mar. Biol. Assoc. UK, 35, 1–33, 1956.

Steele, J. H.: Plant production in the northern North Sea. Scottish Home Dept., Mar. Res., 1958, 1–36, 1958.
Steele, J. H.: Environmental control of photosynthesis in the sea, Limnol. Oceanogr., 7, 137–150, 1962.
Steele, J. H.: The Structure of Marine Ecosystems, Harvard Univ. Press, 128 pp., 1974.
Steele, J. H. and Henderson, E. W.: A simple plankton model, Am. Nat., 117, 676–691, 1981.
Steele, J. H. and Henderson, E. W.: The role of predation in plankton models, J. Plankton Res., 14, 157–172, 1992.
Steele, J. H. and Henderson, E. W.: The significance of interannual variability, in: Towards a Model of Ocean Biogeochemical Processes, edited by: Evans, G. T. and Fasham, M. J. R., Springer Verlag, Heidelberg, 237–360, 1993.
Steele, J. H. and Henderson, E. W.: Predation control of plankton demography, ICES J. Mar. Sci., 52, 565–573, 1995.
Straile, D.: Gross growth efficiencies of protozoan and metazoan zooplankton and their dependence on food concentration, predator-prey weight ratio, and taxonomic group, Limnol. Oceanogr., 42, 1375–1385, 1997.
Thekaekara, M. P. and Drummond, A. J.: Standard values for the solar constant and its spectral components, Nature, 229, 6–9, 1971.
Tsang, C.-F.: The modeling process and model validation, Ground Water, 29, 825–831, 1991.
Vallina, S. M., Simó, R., Anderson, T. R., Gabric, A., Cropp, R., and Pacheco, J. M.: A dynamic model of oceanic sulfur (DMOS) applied to the Sargasso Sea: simulating the dimethylsulfide (DMS) summer paradox, J. Geophys. Res., 113, G01009, doi:10.1029/2007JG000415, 2008.
Vallina, S. M., Ward, B. A., Dutkiewicz, S., and Follows, M. J.: Maximal feeding with active prey-switching: a kill-the-winner functional response and its effect on global diversity and biogeography, Prog. Oceanogr., 120, 93–109, 2014.
Ward, B. A. and Waniek, J. J.: Phytoplankton growth conditions during autumn and winter in the Irminger Sea, North Atlantic, Mar. Ecol.-Prog. Ser., 334, 47–61, 2007.
Ward, B. A., Friedrichs, M. A. M., Anderson, T. R., and Oschlies, A: Parameter optimisation techniques and the problem of underdetermination in marine biogeochemical models, J. Marine Syst., 81, 34–43, 2010.

Ward, B. A., Schartau, M., Oschlies, A., Martin, A. P., Follows, M. J., and Anderson, T. R.: When is a biogeochemical model too complex? Objective model reduction and selection for North Atlantic time-series sites, Prog. Oceanogr., 116, 49–65, 2013.

Weinbauer, M. G.: Ecology of prokaryotic viruses, FEMS Microbiol. Rev., 28, 127–181, 2004.

Wiggert, J. D., Murtugudde, R. G., and Christian, J. R.: Annual ecosystem variability in the tropical Indian Ocean: results of a coupled bio-physical ocean general circulation model, Deep-Sea Res. Pt. II, 53, 644–676, 2006.

Wilson, S. E., Steinberg, D. K., and Buesseler, K. O.: Changes in fecal pellet characteristics with depth as indicators of zooplankton repackaging of particles in the mesopelagic zone of the subtropical and subarctic North Pacific Ocean, Deep-Sea Res. Pt. II, 55, 1636–1647, doi:10.1016/j.dsr2.2008.04.019, 2008.

Wood, S. N. and Thomas, M. B.: Super-sensitivity to structure in biological models, P. Roy. Soc. Lond. B Bio., 266, 565–570, 1999.

Xiao, Y. and Friedrichs, M. A. M.: Using biogeochemical data assimilation to assess the relative skill of multiple ecosystem models in the Mid-Atlantic Bight: effects of increasing the complexity of the planktonic food web, Biogeosciences, 11, 3015–3030, doi:10.5194/bg-11-3015-2014, 2014.

Ye, Y., Völker, C., Bracher, A., Taylor, B., and Wolf-Gladrwo, D. A.: Environmental controls on N_2 fixation by *Trichodesmium* in the tropical eastern North Atlantic Ocean – a model-based study, Deep-Sea Res. Pt. I, 64, 104–117, 2012.

Yool, A., Popova, E. E., and Anderson, T. R.: Medusa-1.0: a new intermediate complexity plankton ecosystem model for the global domain, Geosci. Model Dev., 4, 381–417, doi:10.5194/gmd-4-381-2011, 2011.

Yool, A., Popova, E. E., and Anderson, T. R.: MEDUSA-2.0: an intermediate complexity biogeochemical model of the marine carbon cycle for climate change and ocean acidification studies, Geosci. Model Dev., 6, 1767–1811, doi:10.5194/gmd-6-1767-2013, 2013a.

Yool, A., Popova, E. E., Coward, A. C., Bernie, D., and Anderson, T. R.: Climate change and ocean acidification impacts on lower trophic levels and the export of organic carbon to the deep ocean, Biogeosciences, 10, 5831–5854, doi:10.5194/bg-10-5831-2013, 2013b.

Table 1. Characteristics: published slab models.

reference	location	structure	MLD	irradiance	photosyn.
Evans and Parslow (1985)	Flemish Cap, Subarctic Pacific	NPZ	clim.	astronomical	E&P85
Frost (1987)	Subarctic Pacific	NP(Z)	clim.	data	numeric
Fasham et al. (1990)	Sargasso Sea	2NPZDB{DOM}	clim.	astronomical	E&P85
Robinson et al. (1993)	Pacific upwelling	P2Z	f(winds)	astronomical	numeric?
Fasham (1995)	Subarctic Pacific, North Atlantic	2NPZDB{DOM}	clim.	astronomical	E&P85
Matear (1995)	Subarctic Pacific	2NP2ZDB{DOM}	clim.	data	E&P85
Hurtt and Armstrong (1996)	Sargasso Sea	2NPR	clim.	astronomical	E&P85
Popova et al. (1997)	none (theoretical)	NPZD	hypothet	astronomical	E&P85 E&P85
Anderson and Williams (1998)	English Channel	2NPZDB[DOM]	clim.	astronomical	A93
Spitz et al. (1998)	Sargasso Sea	2NPZDB[DOOM]	clim.	astronomical	E&P85
Fennel et al. (2001)	Sargasso Sea	NPZD	clim.	astronomical	E&P85
Natvik et al. (2001)	Flemish Cap	NPZ	model	astronomical	E&P85
Schartau et al. (2001)	Sargasso Sea	NPZ	1989–93	astronomical	E&P85
Spitz et al. (2001)	Sargasso Sea	2NPZDB[DOM]	1989–93	astronomical	E&P85
Hemmings et al. (2004)	North Atlantic	NPZ	clim.	data	E&P85
Onitsuka and Yanagi (2005)	Japan Sea	NPZD, 2N2P3Z{DOM}	clim.	data	numeric
Findlay et al. (2006)	None (theoretical)	NP	hypothet	none	B&P05
Mitra et al. (2007)	North Atlantic	2NPZDB{DOM}	clim.	astronomical	E&P85
Mitra (2009)	North Atlantic	2NPZDB{DOM}	clim.	astronomical	E&P85
Llebot et al. (2010)	Mediterranean Bay	2N2PD{DOM}	f(R no.)	astronomical	numeric
Kidston et al. (2013)	Southern Ocean	NPZD	model	model	E&P85

MLD: clim. (climatological from data); hypothet. (hypothetical); f(R no.) (function of Richardson number).
Photosynthesis calculation (photosyn.): E&P85 (Evans and Parslow, 1985); A93 (Anderson, 1993); B&P05 (Baoushada and Pascual, 2005).

Table 2. Coefficients for use in Anderson (1993) calculation of light attenuation.

first layer (0–5 m)	second layer (5–23 m)	third layer (> 23 m)
$b_{0,1} = 0.13096$	$b_{0,2} = 0.041025$	$b_{0,3} = 0.021517$
$b_{1,1} = 0.030969$	$b_{1,2} = 0.036211$	$b_{1,3} = 0.050150$
$b_{2,1} = 0.042644$	$b_{2,2} = 0.062297$	$b_{2,3} = 0.058900$
$b_{3,1} = -0.013738$	$b_{3,2} = -0.030098$	$b_{3,3} = -0.040539$
$b_{4,1} = 0.0024617$	$b_{4,2} = 0.0062597$	$b_{4,3} = 0.0087586$
$b_{5,1} = -0.00018059$	$b_{5,2} = -0.00051944$	$b_{5,3} = -0.00049476$

Table 3. Model parameters. Initial settings and fitted model solutions for stations India, Papa and Kerfix (parameters for Biotrans were the same as for India).

param	meaning	unit	initial	India	Papa	Kerfix
$V_P^{\max}(0)$	max. rate photosynthesis 0 °C	$\mathrm{g\,C\,(g\,Chl)^{-1}\,h^{-1}}$	2.0[a]	2.0	1.0	1.0
α	initial slope of P–I curve	$\mathrm{g\,C\,(g\,Chl)^{-1}\,h^{-1}\,(W\,m^{-2})^{-1}}$	0.08[a,b]	0.12	0.12	0.12
k_N	half sat. constant: N uptake	$\mathrm{mmol\,N\,m^{-3}}$	0.5[a,b]	0.5	0.5	0.5
m_P	phyto. mortality (linear)	$\mathrm{d^{-1}}$	0.02[c]	0.02	0.02	0.02
m_{P2}	phyto. mortality (quadratic)	$\mathrm{(mmol\,N\,m^{-3})^{-1}\,d^{-1}}$	0.025[d]	0.025	0.025	0.025
$I_{\max}$	zoo. max ingestion rate	$\mathrm{d^{-1}}$	1.0[a,b]	1.0	1.0	1.4
k_Z	zoo. half saturation for intake	$\mathrm{mmol\,N\,m^{-3}}$	1.0[a,b]	0.52	0.52	0.52
φ_P	grazing preference: P	dimensionless	0.67[a,*]	0.67	0.67	0.67
φ_D	grazing preference: D	dimensionless	0.33[a,*]	0.33	0.33	0.33
β_Z	zoo. absorption efficiency	dimensionless	0.69[e]	0.69	0.69	0.69
k_{NZ}	zoo. net production efficiency	dimensionless	0.75[f]	0.75	0.75	0.75
m_Z	zoo. mortality (linear)	$\mathrm{d^{-1}}$	0.02[c]	0.02	0.02	0.02
m_{Z2}	zoo. mortality (quadratic)	$\mathrm{(mmol\,N\,m^{-3})^{-1}\,d^{-1}}$	0.34[d]	0.34	0.34	0.34
v_D	detritus sinking rate	$\mathrm{m\,d^{-1}}$	5.0[a]	5.0	5.0	5.0
m_D	detritus remineralisation rate	$\mathrm{d^{-1}}$	0.05[a,b]	0.05	0.05	0.05
w_{mix}	cross-thermocline mixing	$\mathrm{m\,d^{-1}}$	0.1[b]	0.1	0.1	0.1
θ_{chl}	C to chlorophyll ratio	$\mathrm{g\,g^{-1}}$	75[g]	75	75	75

References: [a] Fasham (1993); [b] Fasham et al. (1990); [c] Yool et al. (2011, 2013a); [d] Oschlies and Schartau (2005); [e] Anderson (1994); [f] Anderson and Hessen (1995); [g] Oschlies et al. (1999) and Sathyendranath et al. (2009); [*] adjusted for different model structure (see text).

Table 4. Model sensitivity analysis. Variables are: $\mathrm{chl}_{\mathrm{av}}$ (average chlorophyll day 200–300), $\mathrm{chl}_{\mathrm{max}}$ (peak bloom chlorophyll) and N_{min} (minimum nitrate during seasonal drawdown).

parameter	$\mathrm{chl}_{\mathrm{av}}$ $S(p)+10\,\%$	$\mathrm{chl}_{\mathrm{av}}$ $S(p)-10\,\%$	$\mathrm{chl}_{\mathrm{max}}$ $S(p)+10\,\%$	$\mathrm{chl}_{\mathrm{max}}$ $S(p)-10\,\%$	N_{min} $S(p)+10\,\%$	N_{min} $S(p)-10\,\%$
k_Z	0.91	0.98	0.33	0.37	−2.16	−3.02
I_{max}	−0.54	−0.55	−0.59	−0.61	2.97	2.60
φ_P	−0.40	−0.45	−0.17	−0.18	1.30	1.27
k_{NZ}	−0.39	−0.42	−0.55	−0.57	−0.36	−0.04
m_{Z2}	0.28	0.30	0.04	0.04	−0.84	−0.98
β_Z	−0.23	−0.22	−0.55	−0.57	1.90	1.85
α	0.08	0.16	0.14	0.21	−2.56	−3.73
m_P	−0.09	−0.09	0.06	0.08	0.12	0.11
m_D	0.05	005	0.00	0.00	0.55	0.55
m_{P2}	−0.04	−0.04	−0.38	−0.42	0.35	0.36
k_N	−0.04	−0.04	−0.03	−0.03	0.71	0.75
w_{mix}	0.03	0.03	0.00	0.00	0.43	0.43
$V_P^{\mathrm{max}}(0)$	−0.01	0.03	0.21	0.24	−1.84	−2.54
m_Z	0.02	0.02	0.34	0.36	−0.57	−0.60
v_D	−0.01	−0.01	0.00	0.00	−0.49	−0.56

Table C1. Coefficients for use in Anderson (1993) calculation of photosynthesis.

$h_0 = 0.36796$ $h_1 = 0.17537$ $h_2 = -0.065276$
$h_3 = 0.013528$ $h_4 = 0.0011108$
$g_1 = 0.048014$ $g_2 = 0.00023779$ $g_3 = -0.023074$
$g_4 = 0.0031095$ $g_5 = -0.0090545$ $g_6 = 0.0027974$
$g_7 = 0.00085217$ $g_8 = -3.9804 \times 10^{-6}$ $g_9 = 0.0012398$
$g_{10} = -0.00061991$
$\Omega_1 = 1.9004$ $\Omega_2 = -0.28333$ $\Omega_3 = 0.028050$
$\Omega_4 = -0.0014729$ $\Omega_5 = 0.000030841$

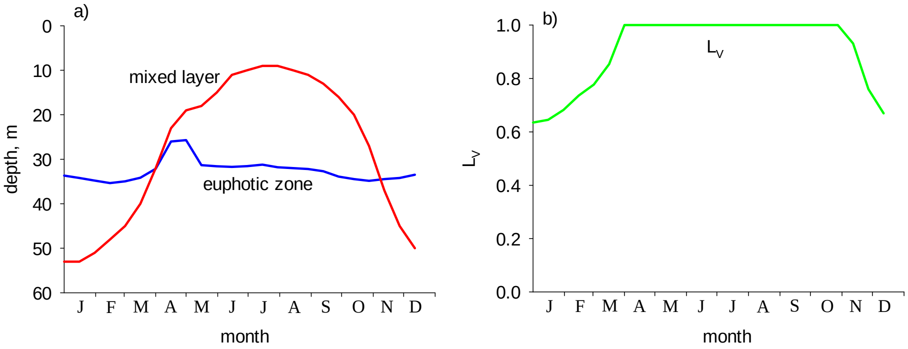

Figure 1. Forcing used by Riley (1946) in his model of George's Bank: **(a)** depths of euphotic zone and mixed layer; **(b)** diminution in photosynthesis due to light limitation (L_V).

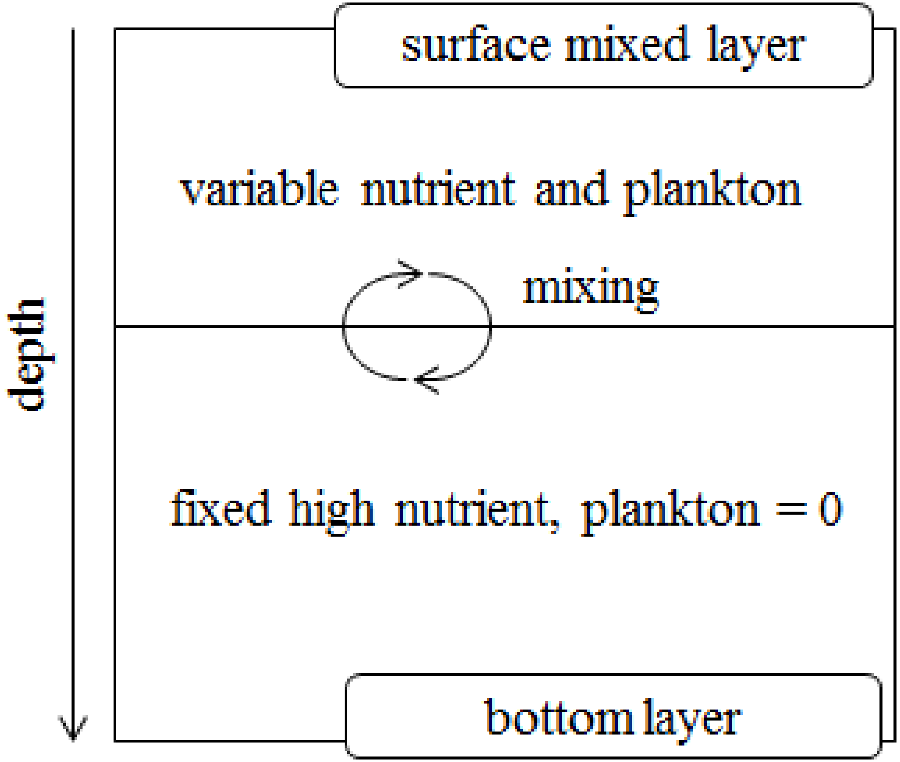

Figure 2. Two layer slab physics framework (adapted from Steele, 1974).

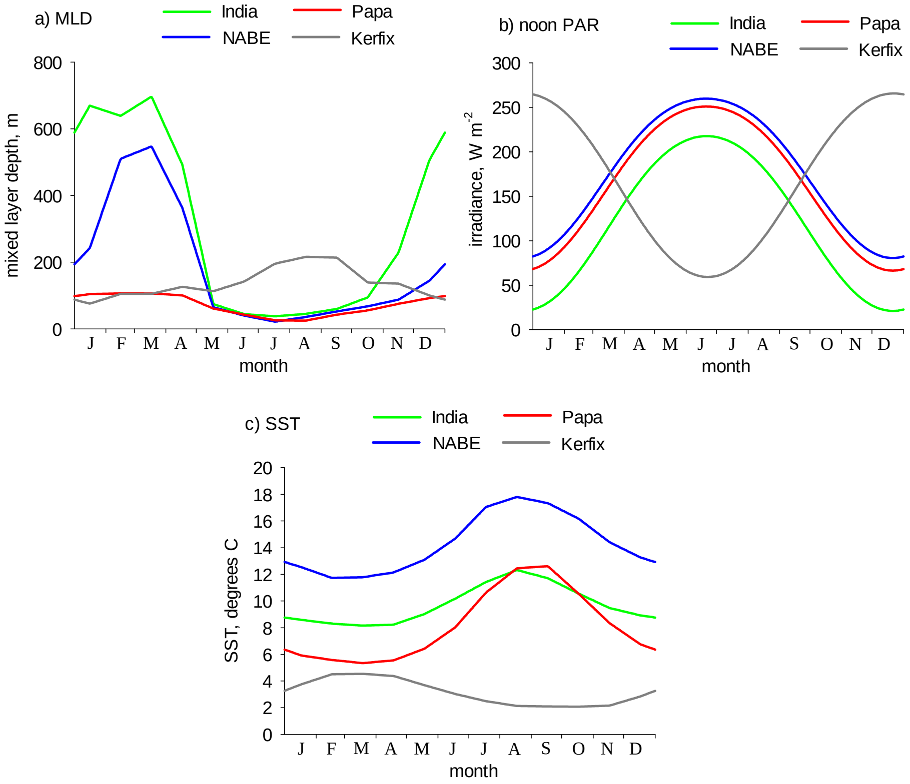

Figure 3. Model forcing for stations India (60° N, 20° W), Biotrans (47° N, 20° W), Papa (50° N, 145° W) and Kerfix (50°40′ S, 68°25′ E): **(a)** mixed layer depth (m), **(b)** noon irradiance (W m^{-2}), **(c)** sea surface temperature (°C).

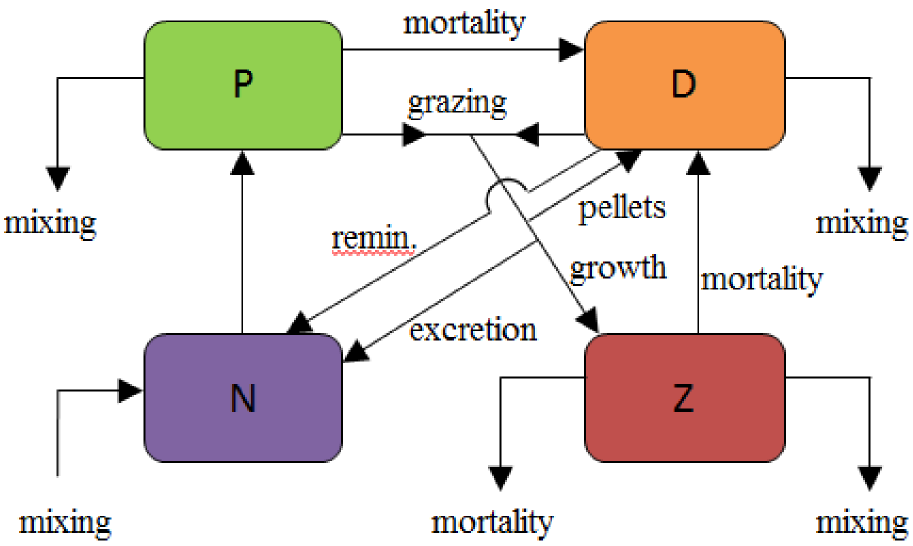

Figure 4. Structure of the NPZD model.

GMDD
8, 53–140, 2015

1.0: an Efficient Model of Planktonic ecOsystems WrittEn in R

T. R. Anderson et al.

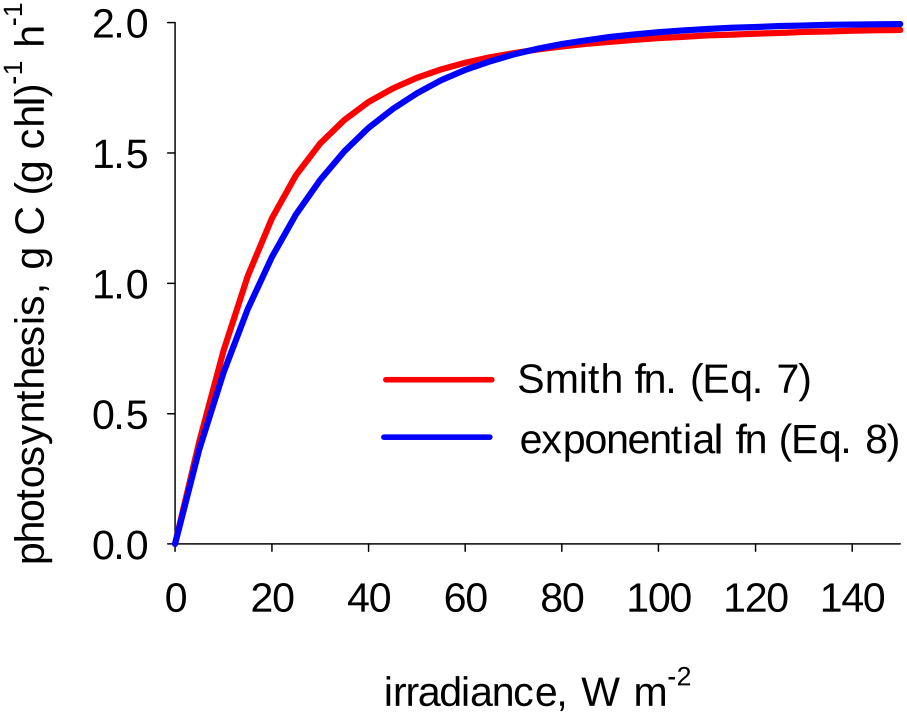

Figure 5. Photosynthesis–irradiance curves with parameter settings: $V_P^{\max} = 2.0\,\mathrm{g\,C\,(g\,Chl)^{-1}\,h^{-1}}$ and $\alpha = 0.08\,\mathrm{g\,C\,(g\,Chl)^{-1}\,h^{-1}\,(W\,m^{-2})^{-1}}$.

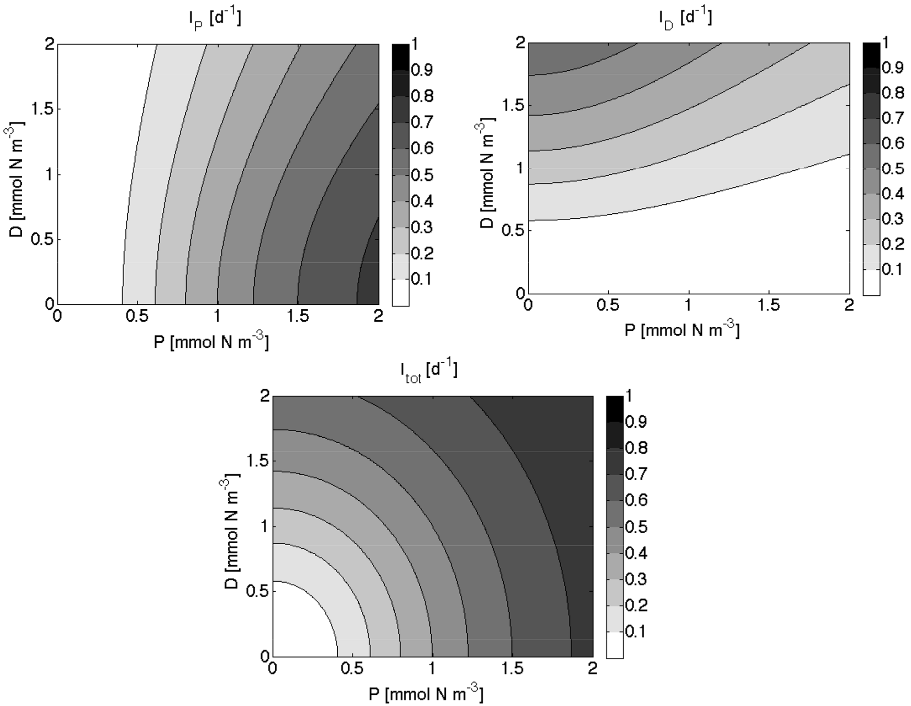

Figure 6. Contours of the zooplankton specific ingestion rates (I_P, I_D) vs. densities of the two prey types (P = phytoplankton and D = detritus) as characterised by the sigmoidal grazing response (Eqs. 11 and 12) using parameters $I_{\text{max}} = 1\,\text{d}^{-1}$, $k_Z = 0.52\,\text{mmol}\,\text{N}\,\text{m}^{-3}$, $\varphi_P = 0.67$ and $\varphi_D = 0.33$. Upper two panels illustrate assumed interference effect of one prey type over another, e.g. for a given P, increasing D reduces I_P. The lower panel illustrates assumed optimal feeding (i.e. total ingestion, I_{tot}, always increases with increase in P or D) and the benefit of generalism (i.e. increase in I_{tot} due to consumption of P and D vs. just P).

Title Page
Abstract
Introduction
Conclusions
References
Tables
Figures
I◀
▶I
◀
▶
Back
Close
Full Screen / Esc
Printer-friendly Version
Interactive Discussion

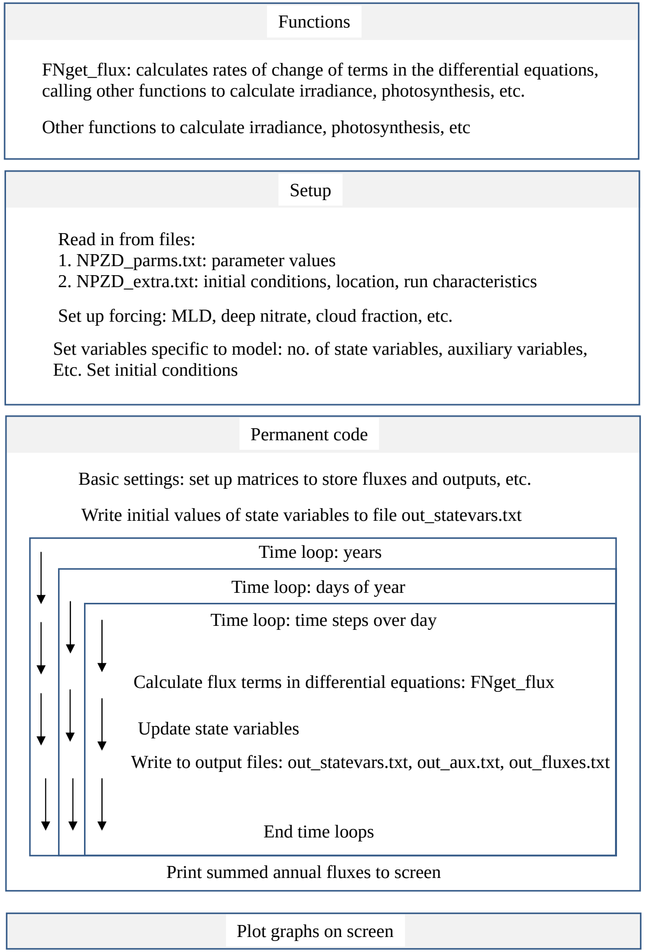

Functions

FNget_flux: calculates rates of change of terms in the differential equations, calling other functions to calculate irradiance, photosynthesis, etc.

Other functions to calculate irradiance, photosynthesis, etc

Setup

Read in from files:
1. NPZD_parms.txt: parameter values
2. NPZD_extra.txt: initial conditions, location, run characteristics

Set up forcing: MLD, deep nitrate, cloud fraction, etc.

Set variables specific to model: no. of state variables, auxiliary variables, Etc. Set initial conditions

Permanent code

Basic settings: set up matrices to store fluxes and outputs, etc.

Write initial values of state variables to file out_statevars.txt

Time loop: years

Time loop: days of year

Time loop: time steps over day

Calculate flux terms in differential equations: FNget_flux

Update state variables

Write to output files: out_statevars.txt, out_aux.txt, out_fluxes.txt

End time loops

Print summed annual fluxes to screen

Plot graphs on screen

Figure 7. Structure of the model code.

Title Page
Abstract | Introduction
Conclusions | References
Tables | Figures
◀| |▶
◀ ▶
Back | Close
Full Screen / Esc
Printer-friendly Version
Interactive Discussion

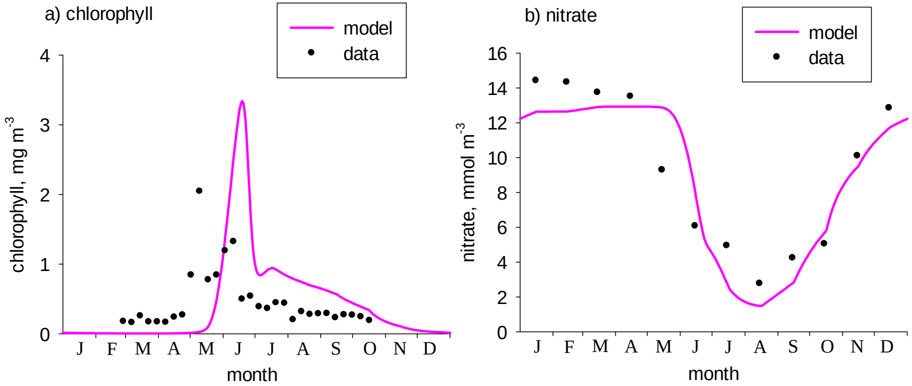

Figure 8. Simulation for station India using first-guess parameters compared to data (year 2006) for **(a)** chlorophyll and **(b)** nitrate.

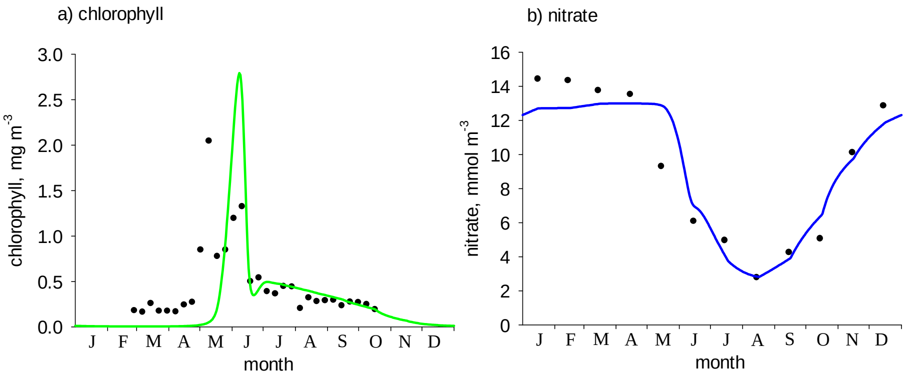

Figure 9. Simulation for station India after parameter tuning (see text): **(a)** chlorophyll, **(b)** nitrate.

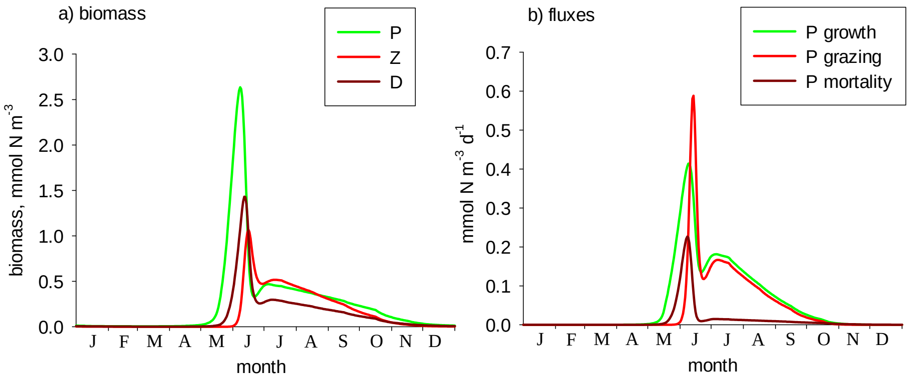

Figure 10. Predicted state variables and fluxes for the station India simulation: **(a)** *P*, *Z* and *D* and **(b)** phytoplankton growth, grazing and non-grazing mortality.

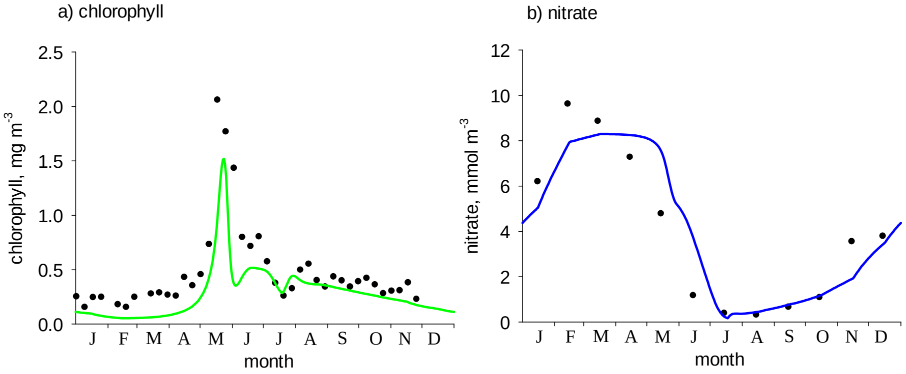

Figure 11. Simulation for station Biotrans: **(a)** chlorophyll, **(b)** nitrate. Data are for year 2008.

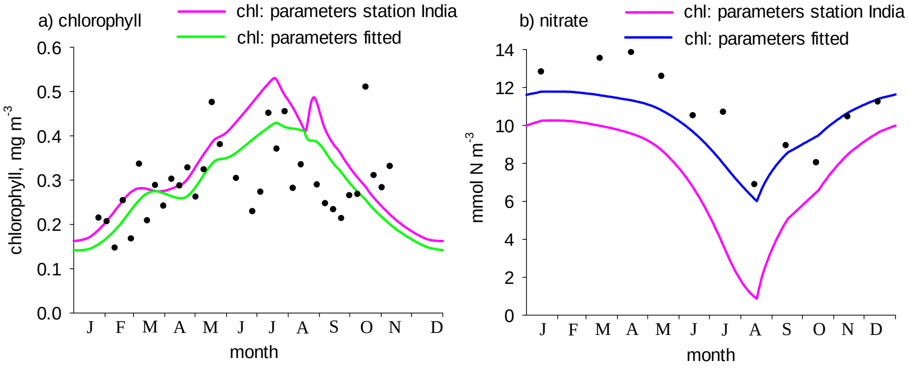

Figure 12. Simulations for station Papa before and after parameter tuning: **(a)** chlorophyll, **(b)** nitrate. Data are for year 2009.

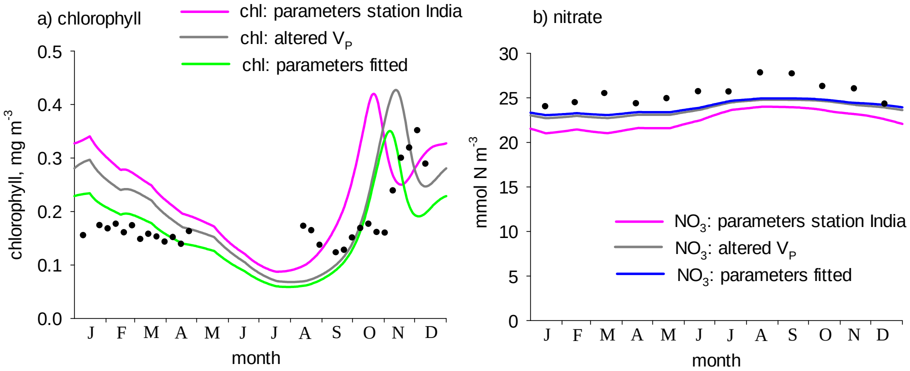

Figure 13. Simulations for station Kerfix before and after parameter tuning (see text for details): **(a)** chlorophyll, **(b)** nitrate. Data are for year 2008.

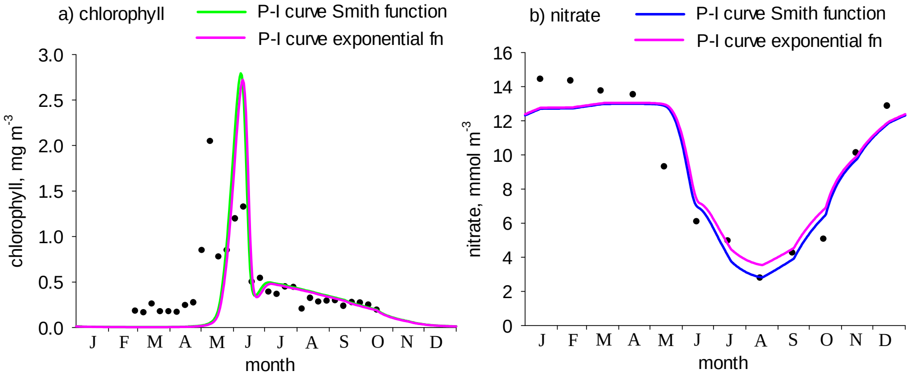

Figure 14. Simulations for station India showing sensitivity to choice of *P–I* curve: **(a)** Smith function (standard run) and **(b)** exponential function.

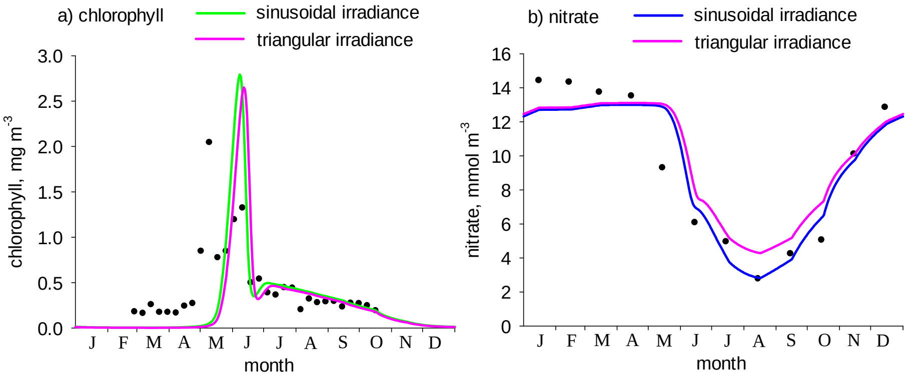

Figure 15. Simulations for station India showing sensitivity to choice of diel variation in irradiance: **(a)** sinusoidal (standard run) and **(b)** triangular.

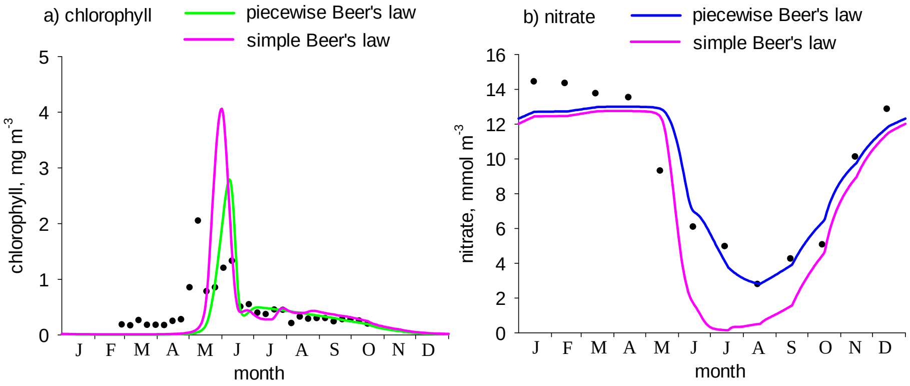

Figure 16. Model simulations for station India showing sensitivity to choice of method for calculating light attenuation in the water column: **(a)** piecewise Beer's Law (Eq. 10) and **(b)** simple Beer's law (Eq. 9).

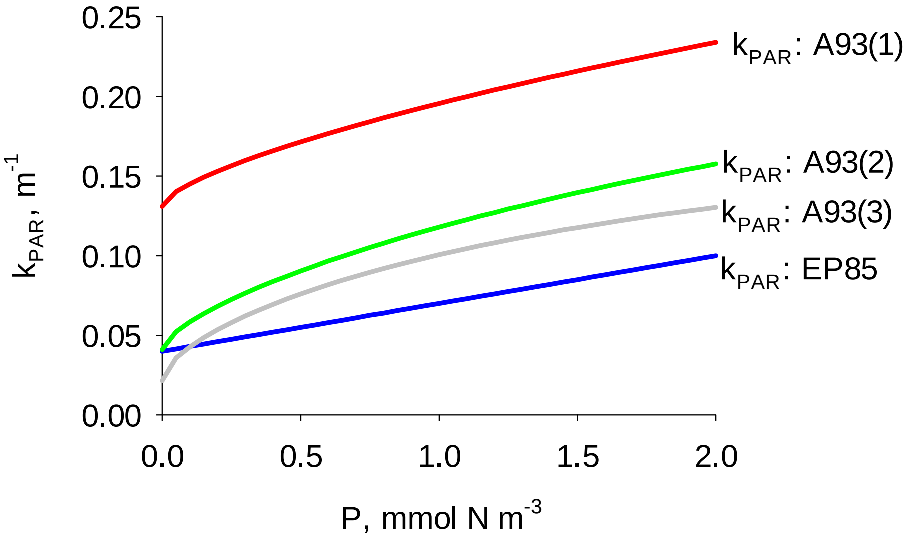

Figure 17. Light attenuation as predicted by Evans and Parslow (1985) and for the three layers (0–5, 5–23, > 23 m; 1, 2, 3 respectively) in Anderson (1993), as a function of phytoplankton concentration.

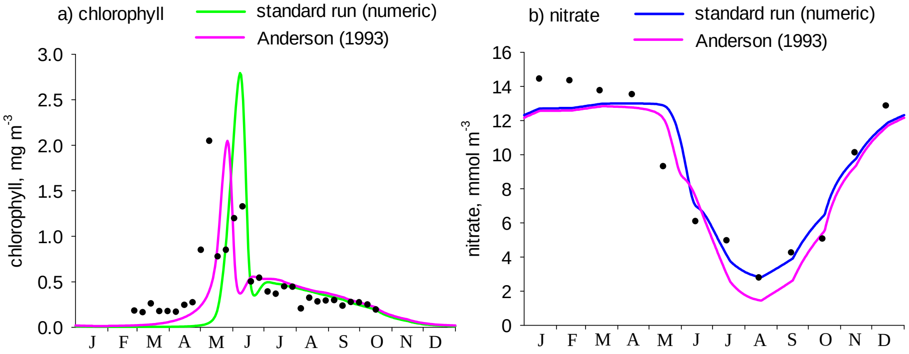

Figure 18. Simulations for station India comparing methods for calculating daily depth-integrated photosynthesis, standard run (numeric integration) and the algorithm of Anderson (1993) which is an empirical approximation of a full spectral model: **(a)** chlorophyll and **(b)** nitrate.

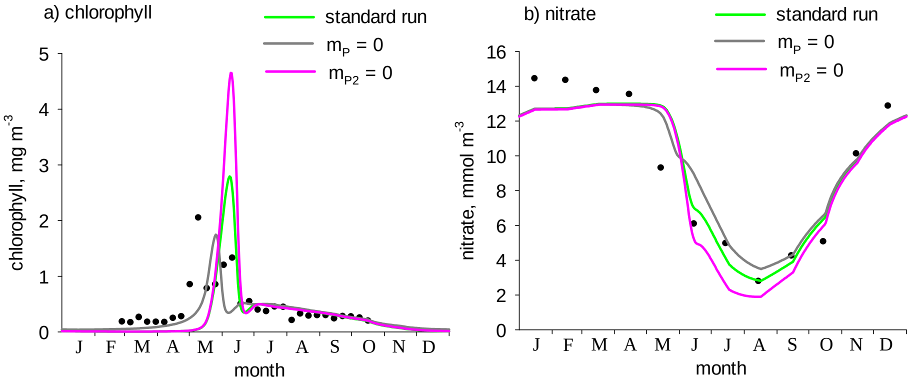

Figure 19. Simulations for station India showing model sensitivity to phytoplankton mortality. Parameters m_P (linear mortality) and m_{P2} (quadratic moratlity) were set to zero in turn. **(a)** chlorophyll, **(b)** nitrate.

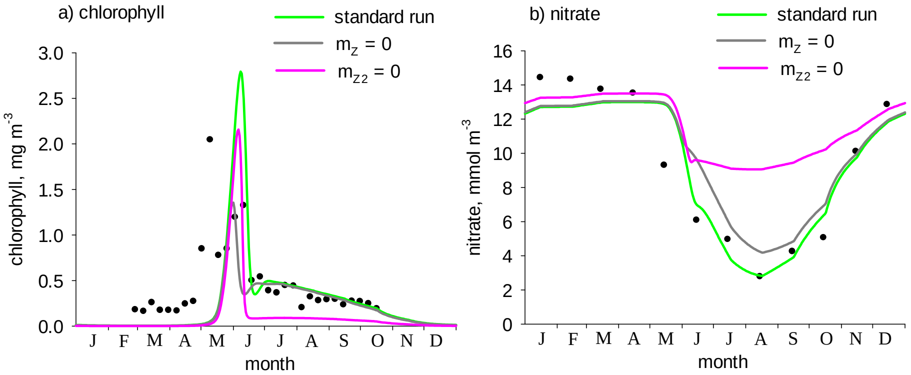

Figure 20. Simulations for station India showing model sensitivity for zooplankton mortality. Parameters m_Z (linear mortality) and m_{Z2} (quadratic moratlity) were set to zero in turn. **(a)** chlorophyll, **(b)** nitrate.